Effects of Serum Amyloid A and Lysophosphatidylcholine on Human Coronary Artery Smooth Muscle Cells: Roles of Transient Receptor Potential Channels

ヒト冠動脈平滑筋における **Serum Amyloid A** 及び **Lysophosphatidylcholine** の生理作用：**TRP** チャネルの役割

田中　悌史

Index

1. Abstract……...**4**

2. Introduction……**5**

3. Method……...**9**

3-1 Cell culture of human coronary artery smooth muscle cells (hCASMCs)……..…**9**

3-2 Solutions and drugs……...……**9**

3-3 Measurement of intracellular Ca^{2+} ($[Ca^{2+}]_i$) and Mg^{2+} ($[Mg^{2+}]_i$) concentration……**9**

3-4 Immunocytochemistry……**10**

3-5 RNA extraction, reverse transcription/polymerase chain reaction (RT-PCR) and real-time quantitative RT-PCR……..……**11**

3-6 Western blotting……..……**12**

3-7 Transfection of synthetic small interfering RNA (siRNA)……..……**12**

3-8 Data analysis……...……**13**

4. Result……**14**

4-1 Effects of SAA and LPC on $[Ca^{2+}]_i$ mobilization in hCASMCs……**14**

4-2 Effects of various drugs on SAA- and LPC-induced $[Ca^{2+}]_i$ rise……..…**19**

4-3 Expression of TRP family mRNA in hCASMCs……**22**

4-4 Expression of TRPC, TRPV4 and TRPM7 protein in hCASMCs……..…**25**

4-5 Effects of LPC on $[Mg^{2+}]_i$ mobilization in hCASMCs……...……**29**

4-6 Effects of preincubation of pertussis and cholera toxin on $[Ca^{2+}]_i$ mobilization...….**31**

4-7 Effects of U73122 on SAA- and LPC-induced $[Ca^{2+}]_i$ rise in hCASMCs……..**31**

4-8 Effects of siRNA for TRPC4 on mRNA level and $[Ca^{2+}]_i$ response to SAA in hCASMCs…….....….……...**34**

5. Discussion…….……...….**36**

6. Acknowledgement…….……...**43**

7. References…….…….…….....**44**

1. Abstract

Background: Serum amyloid A (SAA) and lysophosphatidylcholine (LPC) contribute to physiological processes of atherosclerosis and cardiovascular disease. However, the effects of SAA/LPC on human coronary artery smooth muscle cells (hCASMCs) have not been investigated. Therefore, I examined the effects of SAA/LPC on Ca^{2+}/Mg^{2+} mobilization and its underlying mechanisms in hCASMCs. **Methods:** Intracellular Ca^{2+}/Mg^{2+} concentration ($[Ca^{2+}]_i$ / $[Mg^{2+}]_i$) was measured with fura-2 AM/mag-fura-2 AM. The conventional/real-time quantitative RT-PCR, Western blot and immunocytochemistry were applied. Small interfering RNA (siRNA) for TRPC4 was used to knock down TRPC4. **Result:** SAA/LPC increased $[Ca^{2+}]_i$ by Ca^{2+} entry. The SAA-induced Ca^{2+} entry was inhibited by Gd^{3+}, SKF96365 and 2-aminoethoxydiphenyl borate (2-APB), but not nifedipine. The LPC-induced Ca^{2+} entry was blocked by Gd^{3+}, but not nifedipine, SKF96365 and 2-APB. U73122 and PTX prevented the activation of SAA-, but not LPC-induced Ca^{2+} influx. LPC, but not SAA, increased $[Mg^{2+}]_i$. The RT-PCR, Western blot and immunocytochemistry of TRP channels revealed the expression of TRPC1/4, TRPV1/2/4 and TRPM7. In siRNA treated cells, the level of TRPC4 mRNA was reduced, and Ca^{2+} response for SAA was attenuated, compared with control cells. **Conclusion:** These results suggest that SAA/LPC activate Ca^{2+} influx in hCASMCs; SAA activates it via PTX-sensitive G-protein, PLC and TRPC pathways, where TRPC4 may be involved. On the other hand, LPC may activate it independently of these pathways. TRP protein may be a target molecule of Ca^{2+} signaling in hCASMCs elicited by SAA/LPC, which may play roles in coronary muscle remodeling under the pathophysiological conditions such as atherosclerosis.

2. Introduction

Serum amyloid A (SAA) proteins are a family of apolipoproteins associated with high-density lipoproteins (HDL) in plasma. Its structure has four homologous, alpha-helical proteins encoded by the genes located on chromosome 11 in humans. It consists of SAA1/SAA2, acute phase proteins, and SAA4, which is expressed constitutively. SAA3 is not expressed in humans.[1)] These proteins are produced predominantly by the liver in response to inflammation, but they are also synthesized in endothelial cells, smooth muscle cells and macrophages at the atherosclerotic lesion.[2,3)] The plasma concentration of SAA is normally below 0.08 μM, however, during acute inflammation, interleukin-1 (IL-1), interleukin-6 (IL-6) and tumor necrosis factor (TNF) induce secretion of SAA, resulting in an increase of plasma concentrations more than 40 μM.[4)] Furthermore, the production of SAA by smooth muscle cells and other non-hepatic cells suggests that SAA is not only a sensitive marker of acute inflammatory and atherosclerotic state but contributes to the progression of the inflammation and atherosclerosis. SAA levels have also been reported to be elevated in the patients with atherosclerosis diseases, diabetes and obesity.[5-7)] Johnson et al.[7)] (2004) reported that SAA level is associated with the severity of coronary disease including a number of coronary lesions and diseased coronary branches. SAA has several biological functions in the vascular system. It causes endothelial dysfunction of porcine coronary arteries and human coronary endothelial cells by producing reactive oxygen species, and decreasing eNOS expression.[8)] It also enhances smooth muscle cell migration.[9)] These functions may play a role in remodeling of the vessel under the various conditions including atherosclerosis.

On the other hand, lysphosphatidylcholine (LPC, 1-acyl-sn-glycelo-3-phosphocholine), also called lysolecithin, is a major phospholipid component of oxidized low-density

lipoprotein and is a bioactive proinflammatory lipid. It plays an important role on the atheroscrelosis, acute and chronic inflammation.[10] LPC is a class of chemical compound derived from phosphatidylcholine (PC) of lipoprotein or from cell membrane-derived PC by hydrolyzing PC. The hydrolysis is induced by the enzymatic action of phopholipase A2 (PLA2) and lecithin-cholesterol acyl-transferase (LCAT), which is secreted from the liver and transfers a fatty acid from PC to cholesterol. In plasma, most of the circulating LPC is reversibly bound to albumin, erythrocytes and lipoproteins. And, albumin acts as a reservoir for LPC, effectively controlling LPC bioavailability.[11] Concentrations of LPC in vivo are in the range of 5-180 μM varying in different tissues and body fluids.[12] But, increased concentrations of LPC in blood have been reported in several diseases, such as atherosclerosis, diabetes, hyperlipidemia and obesity.[13-15] LCAT activity levels have also been reported to be increased depending on the severity of coronary atherosclerosis and the changes in the activity of this enzyme are appropriately reflected by an increase of LPC concentration in plasma.[16] Thus, atherosclerotic arteries are chronically exposed to high concentration of LPC as compared with normal arteries.[17,18] LPC-mediated biological effects are diverse on numerous types of cells including coronary artery.[19] LPC impairs endothelium-dependent relaxing factor-mediated vasodilation and inhibits nitric oxide production.[20] It has been also reported to increase reactive oxygen species (ROS) generation, and induce up-regulation of cytokines (IL-1β, IL-6, IL-8), adhesion molecules (intracellular adhesion molecule-1 (ICAM-1), vascular cell adhesion molecule-1 (VCAM-1)), [21-24] growth factors, chemotaxis, migration/proliferation,[21,25] and apoptosis.[26]

Thus, both SAA and LPC are inflammatory substances and contribute to physiological processes that lead to atherosclerosis including endothelial dysfunction. However, the detailed molecular mechanisms participating in the signal transduction are not fully investigated. A

few studies suggest that the change of calcium mobilization induced by SAA and LPC causes several cellular effects.[27,28] Badolato et al. (1995)[27] reported that SAA increases intracellular calcium concentration ($[Ca^{2+}]_i$) via the signaling pathway including Gi protein in human monocytes. On the other hand, while the previous report showed that LPC induces Ca^{2+} influx via L-type Ca^{2+} channels,[29] Terasawa et al. (2002)[30] suggested that LPC activates nonselective cation current, resulting in a rise of $[Ca^{2+}]_i$ in rabbit coronary artery smooth muscle cells. Over the last decade, transient receptor potential (TRP) channels have been focused attention as one of candidates of nonselective cation channels. TRP channels were initially identified in Drosophila, and later found in vertebrates where they are ubiquitously expressed in many cell types and tissues. Mammalian TRP channels comprise six families (TRPC, TRPV, TRPM, TRPP, TRPML, TRPA), and all channels are made of six-transmembrane polypeptide subunits that assemble as tetramers to form cation-permeable pores.[31-33] Several studies suggested the involvement of TRP on LPC-induced $[Ca^{2+}]_i$ rise. TRPC5 could be activated by lysophospholipids in HEK293 cells.[34] So et al. (2005)[35] showed that LPC increased $[Ca^{2+}]_i$ in corporal smooth muscle cells probably through activation of TRPC6. Schilling and Eder (2009)[36] reported that TRPC6 and TRPV1 channel activity is required for LPC-induced human monocyte (THP-1) migration. In addition, LPC has been reported to stimulate prostate cancer cell migration via TRPV2.[37] Thus, the target molecule of LPC on Ca^{2+} entry pathways may be different, depending on cell types or the concentration of LPC used in the study. Furthermore, it remains unanswered with respect to the specific channels activated by LPC in human coronary smooth muscle cells (hCASMCs), which play an important role on atherogenesis. In addition, until now, there has been no study that tried to prove the activation of TRP channel induced by SAA in hCASMCs. Therefore, I focused the effects of SAA and LPC on hCASMCs, and aimed to prove the detailed

underlying signal transduction pathway including TRP channels. Thus, TRP protein appears to be a target molecule of Ca^{2+} signaling in hCASMCs elicited by SAA/LPC, which may play roles in coronary muscle remodeling under the pathophysiological and inflammatory conditions such as atherosclerosis.

In the present study, I showed that SAA and LPC activate Ca^{2+} influx pathways in hCASMCs; SAA activates it via a PTX-sensitive G-protein and PLC, where TRPC4 may be involved. On the other hand, LPC may activate it independently of these pathways. Thus, TRP protein appears to be a target molecule of Ca^{2+} signaling in hCASMCs elicited by SAA and LPC, an inflammatory substance.

3. Method

3-1 Cell culture of human coronary artery smooth muscle cells (hCASMCs)

Human coronary artery smooth muscle cells (hCASMCs) were obtained from the Clonetics Corporation (Palo Alto, CA, USA). Cells were maintained at 37 ˚C under 5 % CO_2 in Smooth Muscle Growth Medium-2 (SmGM-2, Clonetics) containing 5 % fetal bovine serum (FBS), recombinant human epidermal growth factor (rhEGF, 0.5 μg/ml), recombinant human fibroblast growth factor (rhFGF, 1 μg/ml), recombinant human insulin (5 mg/ml), gentamicin (50 μg/ml) and amphotericin-B (0.05 μg/ml). At confluence, the cells were detached using 0.05 % trypsin in 0.02 % EDTA, and cultured into the medium. Medium was replaced more than twice weekly. Cells before confluence at passage 2-5 were detached from culture dish with 0.05 % trypsin in 0.02 % EDTA, and used for later experiments.

3-2 Solutions and drugs

Serum amyloid A (SAA) was obtained from Pepro Tech, Inc. (Rocky Hill, NJ) and dissolved in PBS at a concentration of 1 mg/ml. Lysophosphatidylcholine (LPC, palmitoyl, C16:0) was purchased from Sigma (Poole, UK) and dissolved in PBS at a concentration of 5 mM. Pertussis toxin (PTX, Funakoshi, Japan) and cholera toxin (LIST Biological Laboratories, Inc., Campbell, California, USA) was prepared as a stock solution of 200 μg/ml in H_2O. Fura-2 AM and mag-fura-2 AM were purchased from Sigma.

3-3 Measurement of intracellular Ca^{2+} ($[Ca^{2+}]_i$) and Mg^{2+} ($[Mg^{2+}]_i$) concentration

Intracellular Ca^{2+} concentration was measured by fura-2 fluorescence dual-wavelength excitation method as described previously.[38-40)] Cells were incubated with 2 μM fura-2 AM

for 30 min at 37 ˚C under 5 % CO_2. After fura-2 loading, cells were isolated with 0.25 % trypsin and diluted into 10^5 cells per 1ml Tyrode without Ca^{2+} and with 0.1 mM EGTA. Fluorescence ratio between excitation and emission was continuously measured with constant stirring with intracellular ion analyzer CAF-110 (JASCO Corporation, Japan). Fura-2 fluorescence was measured by excitation at 340 nm and 380 nm and emission at 500 nm.

The selective fluorescent probe, mag-fura-2 AM, was used to measure $[Mg^{2+}]_i$.[41] Cells were loaded with mag-fura-2 AM (4 μM), which was dissolved in dimethyl sulfoxide with 0.02 % pluronic acid. After mag-fura-2 loading, cells were isolated with 0.25 % trypsin and diluted into 10^5 cells per 1ml Tyrode without Mg^{2+} and with 0.1 mM EDTA. Fluorescence ratio between excitation and emission was continuously measured with constant stirring with intracellular ion analyzer CAF-110 (JASCO Corporation, Japan) in a similar manner to fura-2 AM.

3-4 Immunocytochemistry

Immunocytochemistry was performed on cultured hCASMCs using anti-TRP channels antibodies (TRPC1 (Osenses Pty Ltd., Flagstaff Hill, SA, Australia.), TRPC3 (AnaSpec Inc., Femont, CA, USA.), TRPC4 (Alomone Labs Ltd., Jerusalem, Israel.), TRPC6 (Novus Biologicals LLC., Littleton, CO, USA.), TRPV4 (Osenses Pty Ltd., Flagstaff Hill, SA, Australia.), and TRPM7 (Abcam plc., Science Park, Cambridge, UK.)). The cells were cultured on Lab-Tek collagen-coated chamber slide (Nalge Nunc International, Naperville, IL, USA), fixed with 2 % paraformaldehyde in PBS in 20 min, and then blocked for 15 min with 3 % horse serum and 0.1 % saponin in PBS. The cells were incubated for 1 h with primary antibodies diluted with 2 % horse serum and 0.1 % saponin in PBS into 1:200 – 1:1000. For negative controls, cells were treated with normal Rabbit IgG. Alexa Fluor 555 labeled Goat

anti-rabbit IgG antibody diluted 1:1000 (Invitorogen, Carlsbad, CA, USA) was used to visualize the channel expression. The cells were also stained with 2-(4-amidinophenyl)-1*H*-indole-6-carboxamidine (DAPI) to visualize nuclei. A confocal laser scanning microscopy (Olympus Fluo View FV300, Olympus Co., Tokyo) was used for observations.

3-5 RNA extraction, reverse transcription/polymerase chain reaction (RT-PCR) and real-time quantitative RT-PCR

To determine the expression of TRP channels in hCASMCs by RT-PCR, total cellular RNA was extracted from the cultured cells by using the RNeasy mini kit (Qiagen, Cambridge, MA). For RT-PCR, complementary DNA (cDNA) was synthesized from 1 μg of total RNA with reverse transcriptase with random primers (Toyobo, Osaka). The reaction mixture was then subjected to PCR amplification with specific forward and reverse oligonucleotide primers for 35 cycles consisting of heat denaturation, annealing, and extension. The cycling conditions were: denaturation at 98 ˚C for 20 sec, annealing at 52-56 ˚C for 10 sec, extension at 74 ˚C for 1 min. PCR products were size-fractionated on 2 % agarose gels, and stained with ethidium bromide and visualized under UV light. Primers were chosen based on the sequence of human TRP family genes (TRPC1, 3, 4, 5, 6, 7, TRPV1-6, and TRPM1-8) as shown in table 1.

Real-time quantitative RT-PCR was performed with the use of real-time Taq-Man technology and a sequence detector (ABI PRISM®7000, Applied Biosystems, Foster City, CA). Gene-specific primers and Taq-Man probes were used to analyze transcript abundance. The 18S ribosomal RNA level was analyzed as an internal control and used normalize the values for transcript abundance of TRP family genes. The probes used in this study ware

purchased as Assay-on-Demand from Applied Biosystems (Foster City, CA): assay ID Hs00608195_m1 for TRPC1, Hs00162985_m1 for TRPC3, Hs00211805_m1 for TRPC4, Hs00202960_m1 for TRPC5, Hs00395102_m1 for TRPC6, Hs00220638_m1 for TRPC7, and 4310893E for 18S rRNA endogenous control.

3-6 Western blotting

Proteins were separated on a 10 % polyacrylamide gel for 60 min at 200 V, and then transferred to Amersham Hypond-P (GE Healthcare UK Ltd. Buckinghamshire, England) for 60 min at 72 mA with semi-dry method. After the transfer, the membrane was blocked with 2-3 % skim milk in PBS (0.01 M phosphate buffer, 0.138 M NaCl, 0.027 M KCl, pH 7.4) with 0.1 % Tween 20 (PBS-T) at room temperature for 1 h. The membrane was then exposed to anti-TRPC1, TRPC4, TRPV4, TRPM7 antibody at the dilutions in blocking buffer overnight at 4 ˚C. Then probed membrane was washed three times in PBS-T for 15 min each time, and subsequently incubated with anti-rabbit IgG linked to peroxidase (Santa Cruz Biotechnology, Inc., Santa Cruz, CA, USA.) diluted to 1:5000 with blocking buffer for 1 h at room temperature. After three additional washes, bound antibodies were detected by Chemi-Lumi One Super (Nacalai Tesque, Kyoto, Japan) and analyzed with an LAS-3000 mini image analyzer (Fuji-Film, Tokyo, Japan).

3-7 Transfection of synthetic small interfering RNA (siRNA)

TRPC4 siRNA and nonsilencing (negative control) siRNA as described in table 1 were purchased from Qiagen (Cambridge, MA, USA). They were transfected into hCASMCs to a final concentration of 40 nM, using the Lipofectamine 2000 (2 μl/ml in culture medium; Invitrogen) according to the instructions of the manufacturer. Transfected cells were incubated

for 48 h in an atmosphere of 5 % CO_2 and 95 % air at 37 °C before each experiment. Then, analysis of mRNA by using real-time RT-PCR, and Ca^{2+} response for SAA was examined.

3-8 Data analysis

All values are expressed as means ± S.E.M. Differences between groups were compared by ANOVA. When differences were indicated, a Bonferroni's comparison was used to determine significance. Two-group analysis was performed with a Student t-test. Differences were considered significant if $P<0.05$.

4. Results

4-1 Effects of SAA and LPC on $[Ca^{2+}]_i$ mobilization in hCASMCs

The effects of SAA and LPC on $[Ca^{2+}]_i$ were investigated, by using Ca^{2+}-sensitive dye fura 2-AM. As shown in Figure 1A, both SAA (10 μg/ml, Figure 1Aa) and LPC (10 μM, Figure 1Ab) increased $[Ca^{2+}]_i$ in the presence of extracellular Ca^{2+}. The SAA-induced $[Ca^{2+}]_i$ rise quickly returned to a near control level within several minutes (Figure 1Aa), while LPC induced a sustained rise in $[Ca^{2+}]_i$ in the presence of extracellular Ca^{2+} (Figure 1Ab). After the SAA-induced $[Ca^{2+}]_i$ rise returned to a control level, the additional application of LPC induced a sustained rise $[Ca^{2+}]_i$ (Figure 1Ac). On the other hand, in a cell bathed into the Ca^{2+}-free standard solution, SAA (10 μg/ml, Figure 1B) failed to increase $[Ca^{2+}]_i$. The subsequent application of histamine (100 μM) transiently increased $[Ca^{2+}]_i$ due to Ca^{2+} release from intracellular store sites, suggesting that SAA-increased $[Ca^{2+}]_i$ rise was mainly due to the entry of extracellular Ca^{2+}.

The effects of extracellular Ca^{2+} on LPC-induced $[Ca^{2+}]_i$ rise were investigated in Figure 1C. In the absence of extracellular Ca^{2+}, LPC (10 μM) only slightly increased $[Ca^{2+}]_i$, but the addition of Ca^{2+} into the bath solution markedly induced a sustained rise in $[Ca^{2+}]_i$ due to Ca^{2+} entry (Figure 1Ca). On the other hand, in the absence of LPC, the Ca^{2+} entry was minimal (Figure 1Cb). These results suggest that LPC induced Ca^{2+} entry in hCASMCs as reported in rabbit coronary artery smooth muscle cells previously.[30)]

Figure 2 shows the concentration-dependent effects of SAA on $[Ca^{2+}]_i$. SAA (Figure 2A, 0.1-10 μg/ml) transiently increased $[Ca^{2+}]_i$ in a concentration-dependent manner. Concentration-dependency of SAA was shown in Figure 2B (n=4). SAA at concentrations above 0.3 μg/ml significantly increased $[Ca^{2+}]_i$ in a concentration-dependent manner.

Figure 3 illustrates the concentration-dependent effects of LPC on $[Ca^{2+}]_i$. Since LPC at high concentrations more than 50 μM has been known to induce a toxic and detergent effect, we have tested the concentration lower than 25 μM. As shown in Figure 3A, LPC (n=5, 3-25 μM) significantly increased $[Ca^{2+}]_i$ in a concentration-dependent manner. Concentration-dependency of LPC was presented in Figure 3B. LPC at concentrations above 3 μM increased $[Ca^{2+}]_i$ in a concentration-dependent manner.

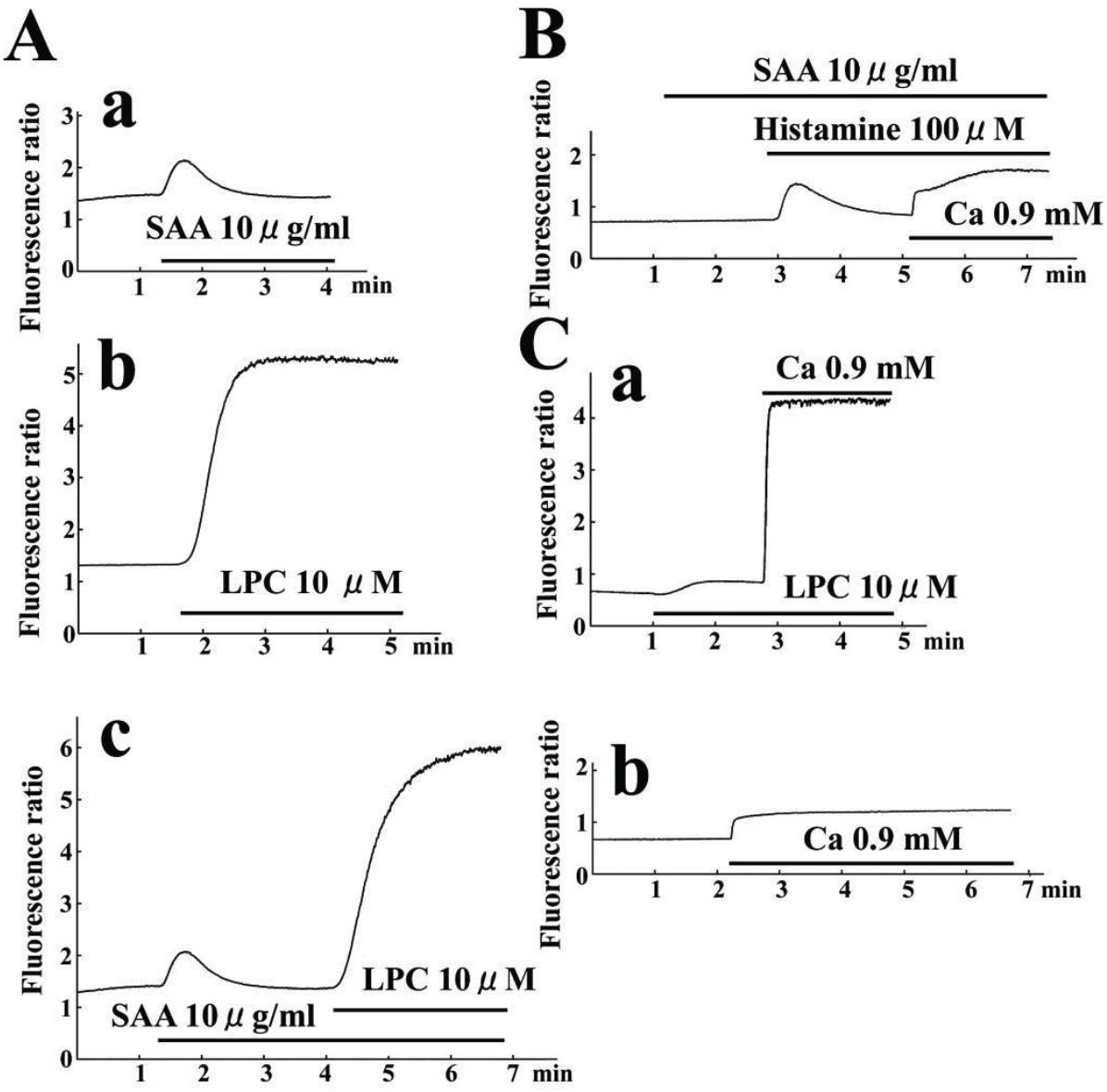

Figure 1. Effects of SAA and LPC on $[Ca^{2+}]_i$ in hCASMCs.

The Ca^{2+}-free bathing solution contained 0.1 mM EGTA in the absence of extracellular Ca^{2+}. 0.9 mM Ca^{2+} was added into the solution to obtain Ca^{2+}-containing solution. A: Effects of SAA (Aa and Ac, 10 μg/ml) and LPC (Ab and Ac) in the presence of extracellular Ca^{2+}. Note that SAA transiently increased $[Ca^{2+}]_i$, and LPC induced a sustained rise in $[Ca^{2+}]_i$. B: Effects of SAA and histamine in the absence of extracellular Ca^{2+}. Note that SAA failed to increase $[Ca^{2+}]_i$, but the additional application of histamine transiently increased $[Ca^{2+}]_i$ due to Ca^{2+}-release from Ca^{2+} store sites. C: Effects of LPC on $[Ca^{2+}]_i$. The $[Ca^{2+}]_i$ rise elicited to Ca^{2+} entry due to the addition of Ca^{2+} was compared in a cell bathed with LPC (10 μM, Ca) or without LPC (Cb). Note that LPC only slightly increased $[Ca^{2+}]_i$, but the additional application of Ca^{2+} markedly increased $[Ca^{2+}]_i$ due to Ca^{2+} entry. The data were representative of three different experiments.

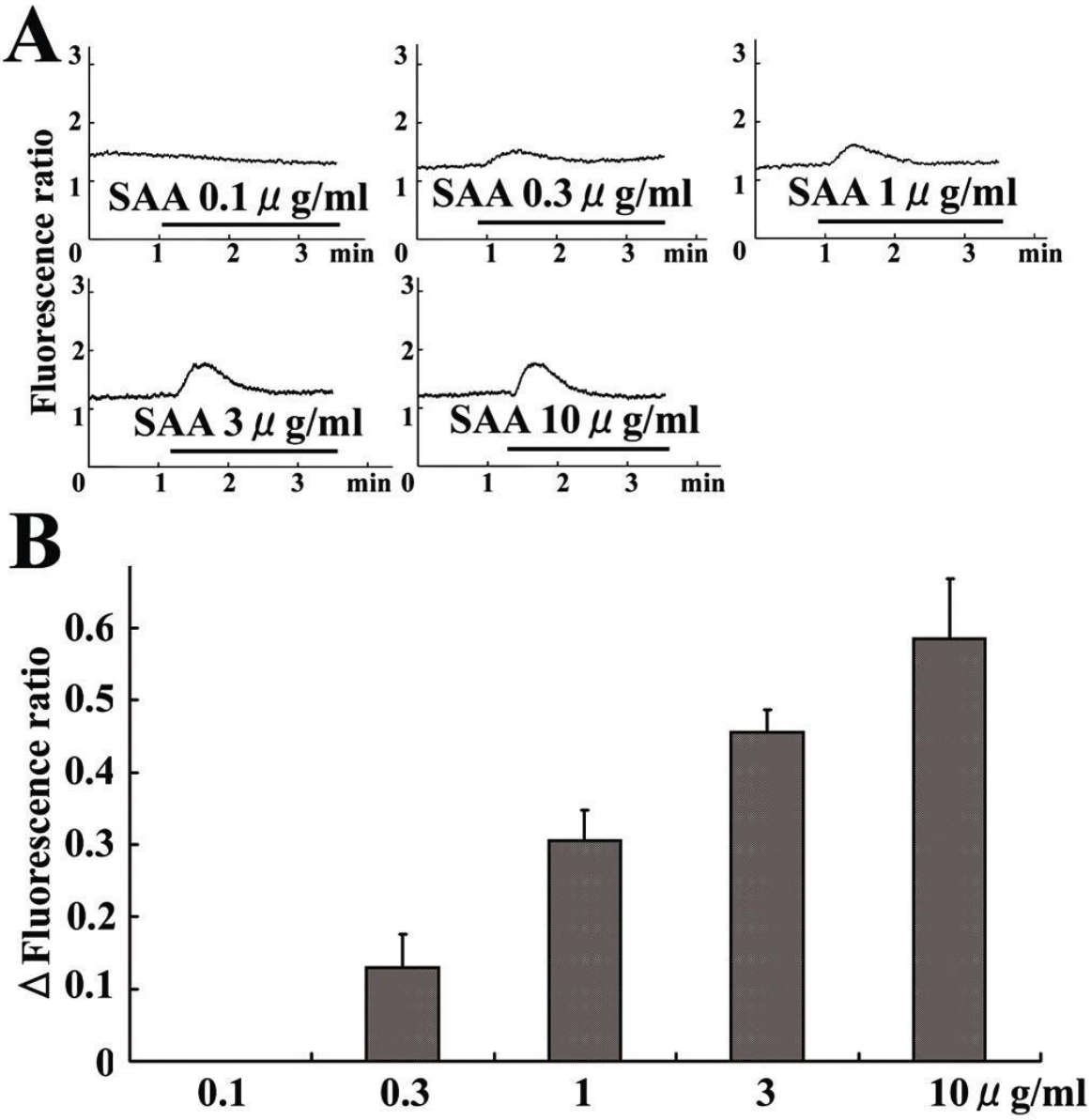

Figure 2. Concentration-dependent effects of SAA on $[Ca^{2+}]_i$ in hCASMCs.

The original data are shown in A. B: Concentration-dependent effects of SAA (0.1-10 μg/ml). The increased fluorescence ratio at the peak level relative to the basal level was plotted against each concentration of SAA. The data were obtained from 4 preparations

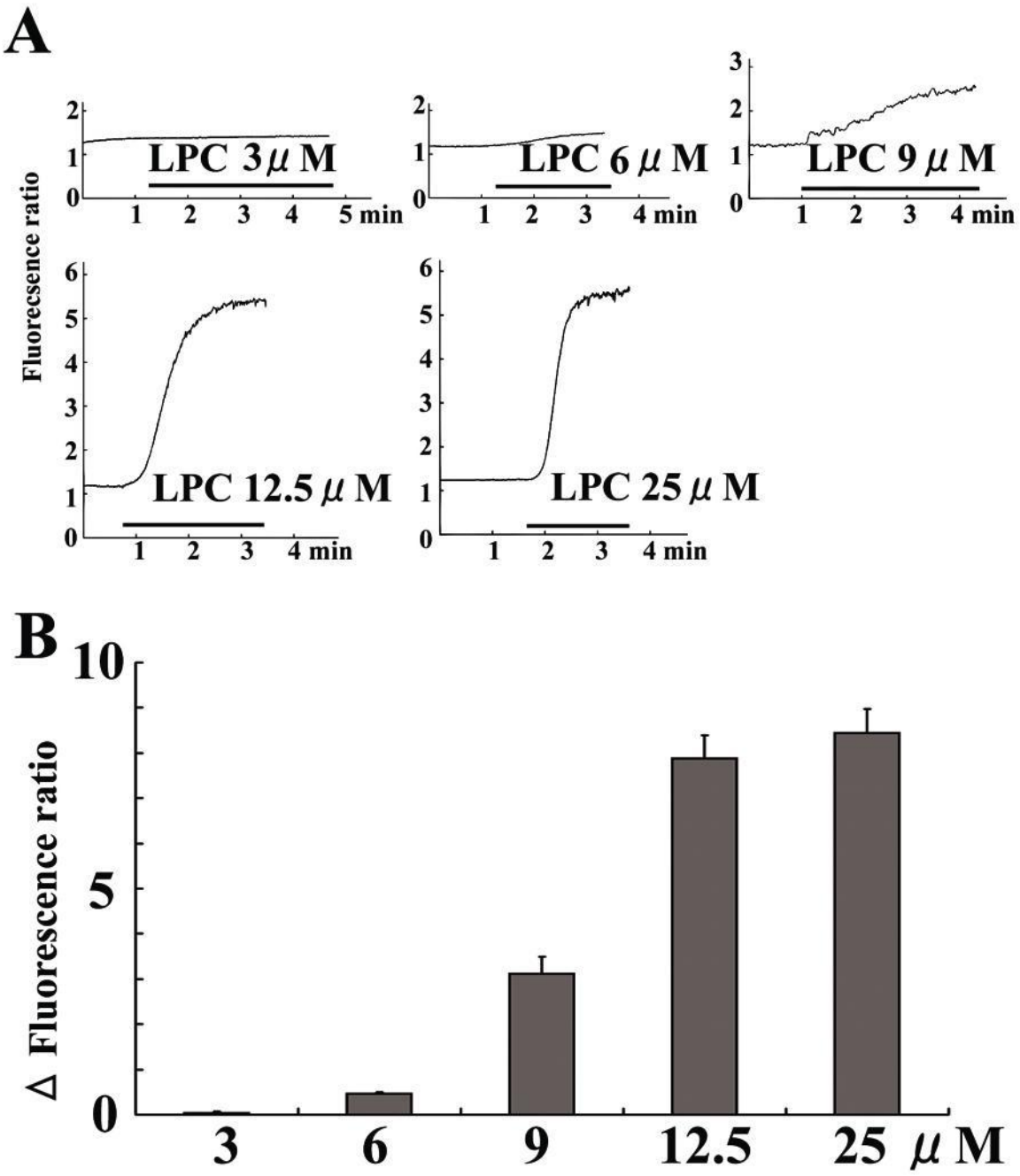

Figure 3. Concentration-dependent effects of LPC on $[Ca^{2+}]_i$ in hCASMCs.
The original data are shown in A. B: Concentration-dependent effects of LPC (3-25 μM). The increased fluorescence ratio at the peak level compared with the basal level was plotted against each concentration of LPC. The data were obtained from 5 preparations.

4-2 Effects of various drugs on SAA- and LPC-induced $[Ca^{2+}]_i$ rise

The above results suggest that SAA and LPC increase $[Ca^{2+}]_i$ mainly via enhancement of Ca^{2+} entry. Therefore, I investigated whether several blockers inhibit calcium mobilization induced by SAA and LPC. First, I added 10 μM nifedipine, a L-type Ca^{2+} channel blocker, into the cuvette before the addition of extracellular calcium (0.9 mM) and SAA or LPC. As shown in Figures 4Aa and 4Ab, inclusion of 10 μM nifedipine in the bath solution did not significantly affect SAA- and LPC-induced $[Ca^{2+}]_i$ rise (Figure 4Ab), compared with the control cells (Figure 4Aa), suggesting that L-type Ca^{2+} channel does not significantly contribute to the Ca^{2+} rise. Similarly, mibefradil (10 μM), a T-type Ca^{2+} channel blocker, did not affect the SAA- and LPC-induced $[Ca^{2+}]_i$ rise (Figures 4B and C). These results suggest that L-type and T-type calcium channels don't participate in SAA- and LPC-induced $[Ca^{2+}]_i$ rise.

Therefore, to further determine the type of channels involved in calcium influx, I next examined the effects of relatively non-specific TRP channel blocker, Gd^{3+} (100 μM, Figure 4Ac). Both SAA (10 μg/ml) and LPC (10 μM) failed to increase $[Ca^{2+}]_i$ in a cell pretreated with Gd^{3+} (100 μM, Figure 4Ac). These results suggest that LPC as well as SAA increase $[Ca^{2+}]_i$ via a non-voltage-dependent Ca^{2+} channel such as TRP, and the toxic or detergent effect of LPC is unlikely. Furthermore, the effects of various drugs on SAA- and LPC-induced $[Ca^{2+}]_i$ rise were also investigated. I used 2-aminoethoxydiphenyl borate (2-APB) and SKF96365, some blockers of TRP channels. Pretreatment of 2-APB (300 μM, Figure 4Ad) or SKF96365 (50 μM, Figure 4Ae) significantly inhibit SAA-induced $[Ca^{2+}]_i$ rise, while it failed to inhibit LPC-induced $[Ca^{2+}]_i$ rise. The inhibitory effects of various blockers are summarized in Figures 4B and 4C. SKF96365 almost completely abolished SAA-induced Ca^{2+} mobilization. Similarly, 300 μM 2-APB reduced it by 81.3 ± 5.4 % of the control (n=3). In

contrast, pretreatment of 2-APB (300 μM, Figure 4Ad) or SKF96365 (50 μM, Figure 4Ae) did not significantly inhibit LPC-induced $[Ca^{2+}]_i$ rise at all.

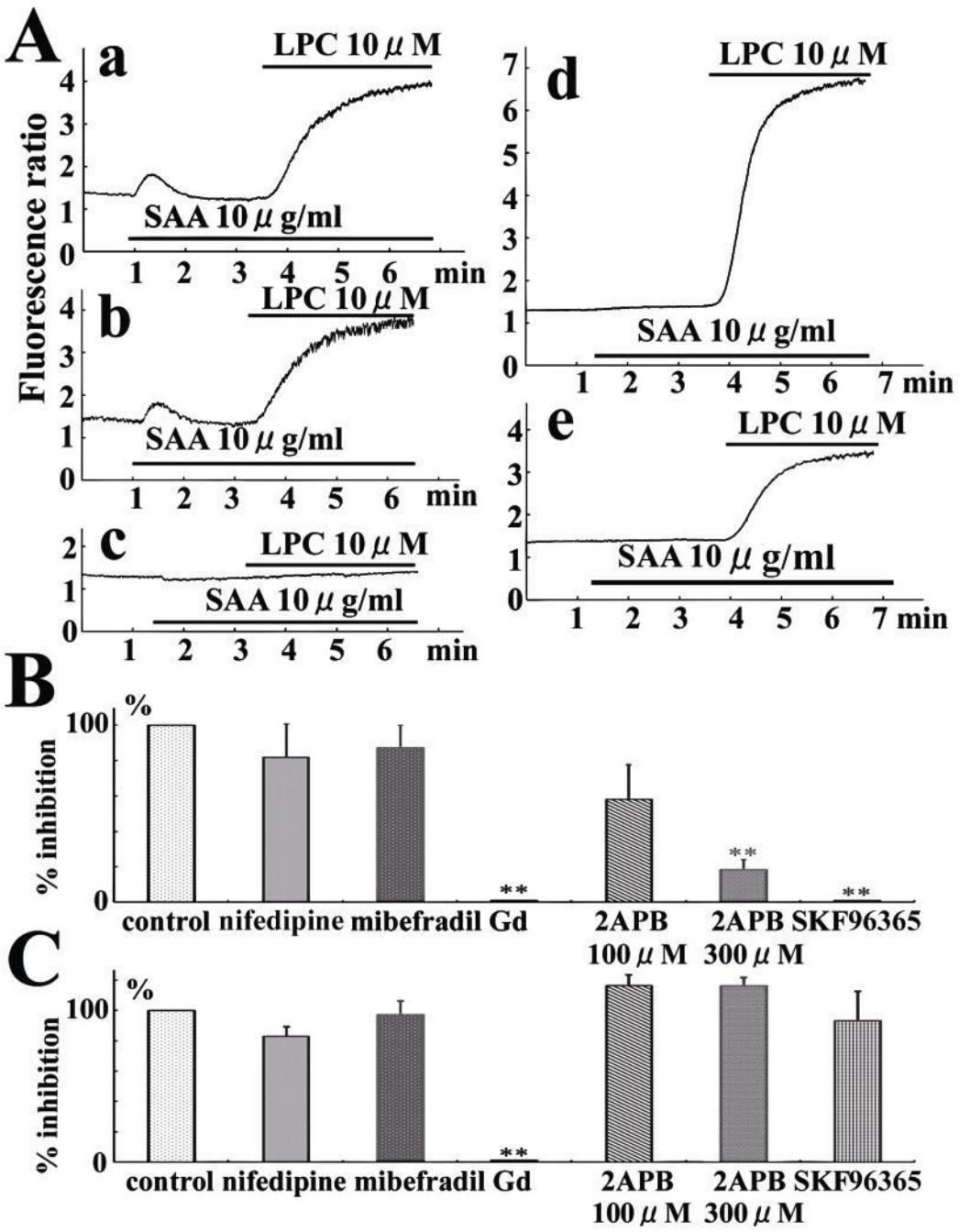

Figure 4. Effects of various drugs on SAA- and LPC-induced $[Ca^{2+}]_i$ rise. The cells were pretreated with various drugs, and then SAA and LPC were added into the control solution. The $[Ca^{2+}]_i$ response was compared with the control cells (untreated with these agents). The typical data are illustrated in A. a: control cells, b: nifedipine (10 μM), c: Gd^{3+} (100 μM), d: 2-aminoethoxydiphenyl borate (2-APB, 300 μM), e: SKF96365 (50 μM). Note that pretreatment of 2-APB (300 μM) or SKF96365 (50 μM) significantly inhibit SAA-induced $[Ca^{2+}]_i$ rise. The data were representative of three different experiments. B and C: The inhibitory effects of various blockers on SAA- and LPC-induced $[Ca^{2+}]_i$ rise. The relative amplitude of SAA (B)- and LPC (C)- induced $[Ca^{2+}]_i$ rise are plotted in each drug, compared with control cells (without drug). The data were obtained from three different cells. **P<0.01 vs. control

4-3 Expression of TRP family mRNA in hCASMCs

I investigated the expression of TRP channel gene members including TRPC, TRPV, and TRPM in hCASMCs (Figure 5, left part). Mouse adult brain was used as a positive control (right part). Figures 5A, 5B, and 5C show the RT-PCR analysis of the transcripts of TRPC1-C7, TRPV1-V6 and TRPM1-8, respectively. Among TRPCs, TRPC2 is a pseudo gene in Homo sapiens, and therefore, I investigated the expression of TRPC1, TRPC3, TRPC4, TRPC5, TRPC6 and TRPC7. TRPC1 and TRPC4 mRNA were detected in hCASMCs, as compared with mouse adult brain. The amplitude of cDNA fragments was of predicted molecular size, identical to cDNA fragments amplified from reversely transcripted mRNA. Among TRPV1-6, TRPV1, TRPV2 and TRPV4 were detected in hCASMCs, but TRPV3, TRPV5, TRPV6 were not detected. The only significant expression of TRPM7 and TRPM8 was observed among TRPMs, while TRPM1, TRPM2, TRPM3, TRPM4, TRPM5 and TRPM6 mRNA were not detected.

The expression of TRPC family mRNA members was also investigated by real-time quantitative RT-PCR analysis (Figure 6). Transcript levels were normalized to 18S ribosomal housekeeping gene. Significant expression of TRPC1 and TRPC4 mRNA was observed, while TRPC3, TRPC5, TRPC6 and TRPC7 mRNA were not detected significantly by real-time quantitative RT-PCR analysis. Thus TRPC1 and C4 appeared to dominantly encode for TRPC channel gene in hCASMCs.

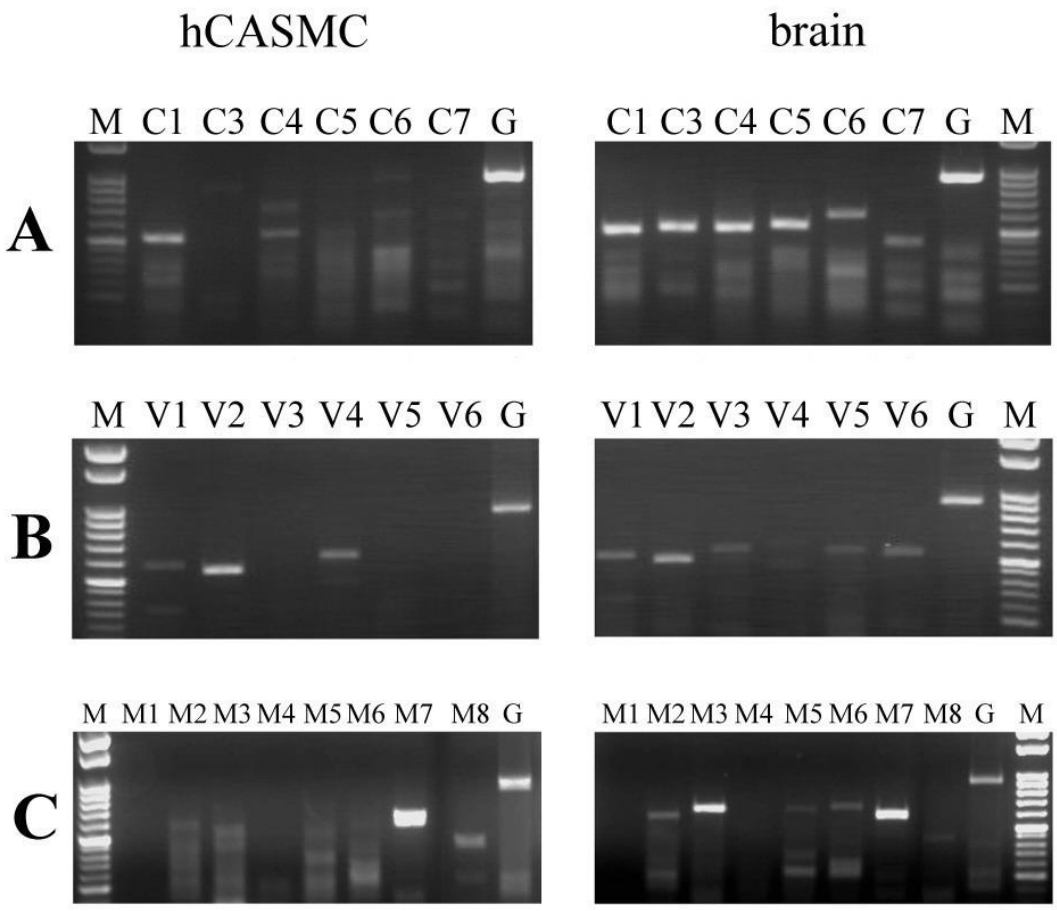

Figure 5. Expression of α subunit gene of TRP channel members including TRPC, TRPV, and TRPM in hCASMCs (left part) and mouse adult brain (right part).

A: TRPC channel mRNA members. Marker (M), TRPC1, TRPC3, TRPC4, TRPC5, TRPC6, TRPC7, GAPDH (G). Note that TRPC1 and TRPC4 were detected in hCASMCs, as compared with mouse adult brain. B: TRPV channel mRNA members. TRPV1, TRPV2, TRPV3, TRPV4, TRPV5, TRPV6. C: TRPM7 channel mRNA members. TRPM1, TRPM2, TRPM3, TRPM4, TRPM5, TRPM6, TRPM7, TRPM8.

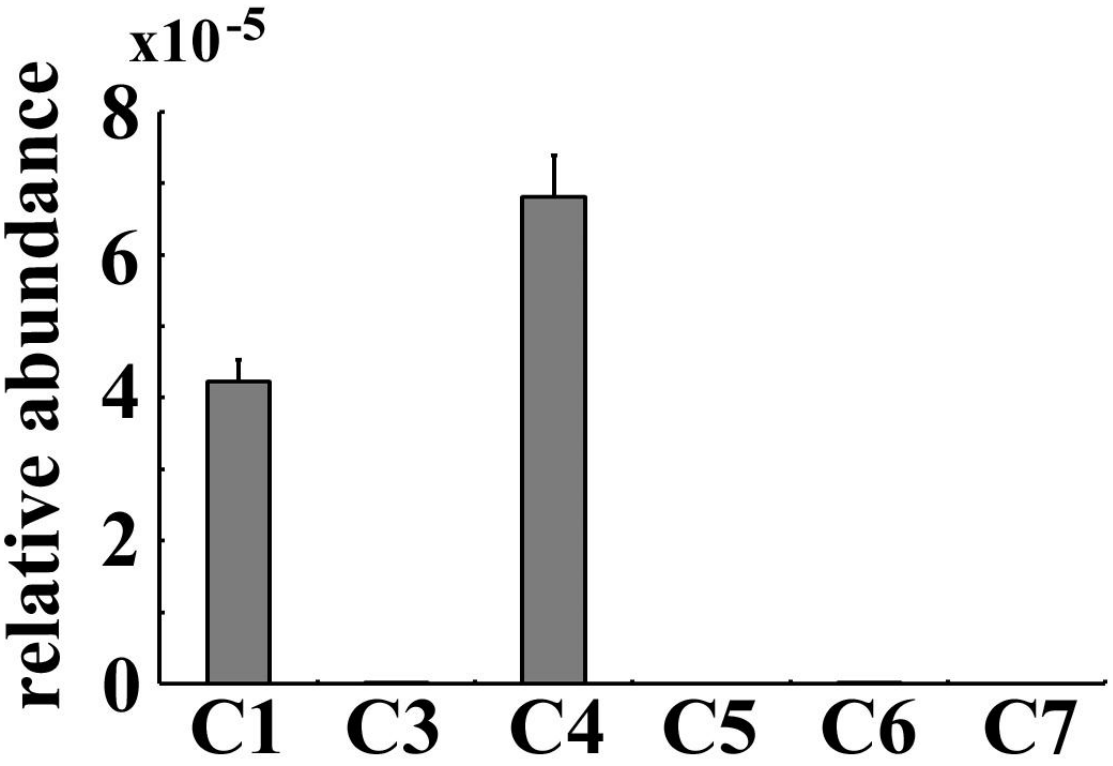

Figure 6. Real-time quantitative RT-PCR analysis of TRPC channel mRNA members in hCASMCs.

The expression levels of TRPC channel genes were normalized to those of the 18S ribosomal RNA levels. Note that dominant expression of TRPC1 and TRPC4 was observed in hCASMCs.

4-4 Expression of TRPC, TRPV4 and TRPM7 protein in hCASMCs

Expression of TRPC1 (Figure 7A), TRPC4 (Figure 8Aa), TRPV4 (Figure 7C) and TRPM7 (Figure 9Aa) was confirmed by immunocytochemistry in hCASMCs. But the expression of TRPC6 was not detected (Figure 7B). The cells were also counterstained with DAPI to visualize nuclei, and double staining of nucleus and TRP channels protein as shown in Figure 7. No expression was detected in negative controls with normal rabbit IgG instead of a primary antibody (Figures 7D, 8Ab and 9Ab).

To confirm TRPC1 (Figure 7A), C4 (Figure 8B), TRPV4 (Figure 7C) and TRPM7 (Figure 9B) protein expression, I also examined hCASMCs lysates by Western blot analysis. A specific antibody for each of the TRP channel protein revealed a strong band.

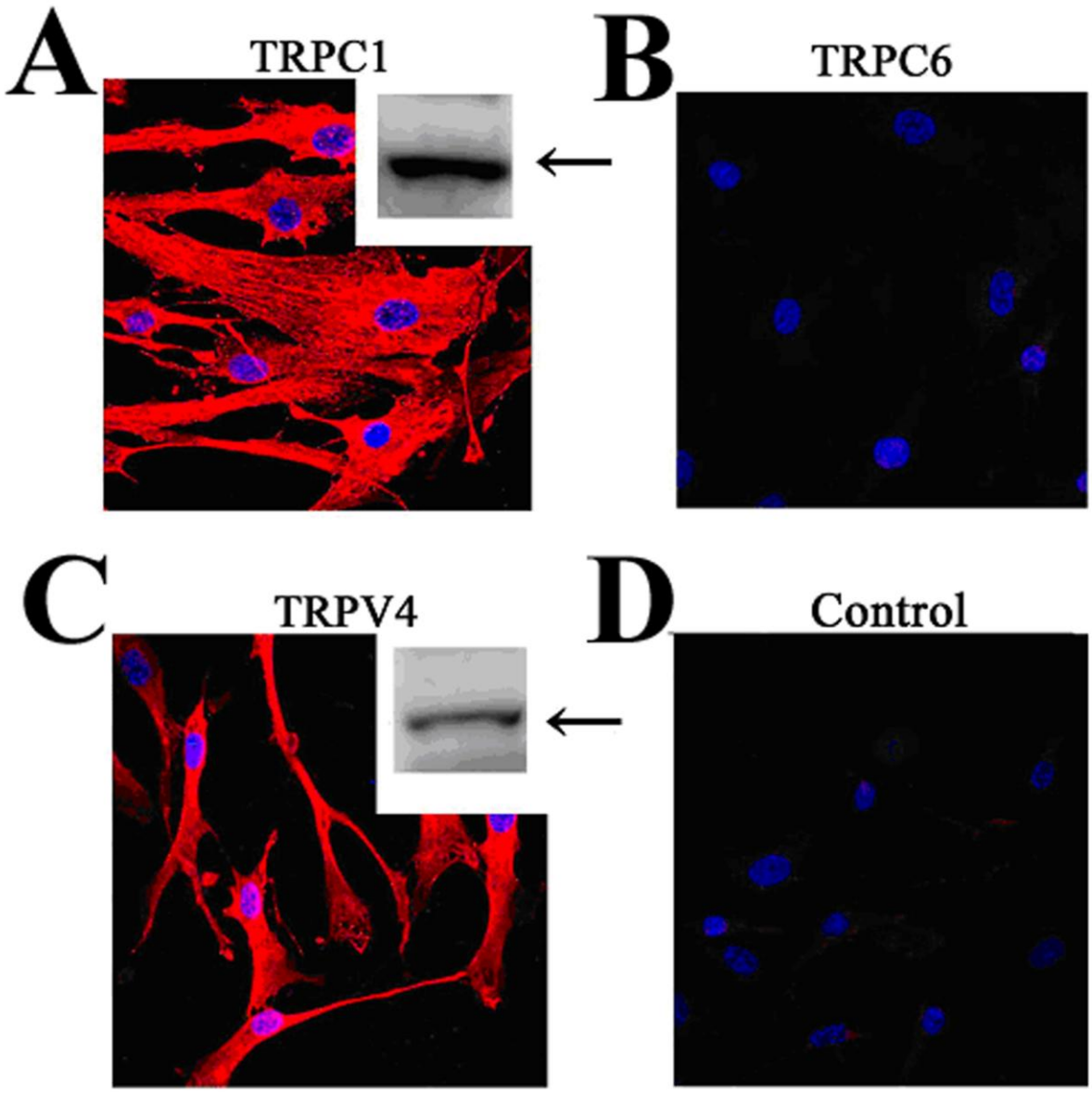

Figure 7. TRPC1, C6 and TRPV4 expression in hCASMCs.
Immunostaining for TRPC1 (A), TRPC6 (B), TRPV4 (C). Negative control without the antibody (D). Double staining of nuclei DAPI to visualize nuclei is illustrated. Note that hCASMCs have significant expression for TRPC1 and TRPV4, compared with TRPC6. Western blotting for TRPC1 and TRPV4 (indicated by an arrow) is shown in the upper part of each picture.

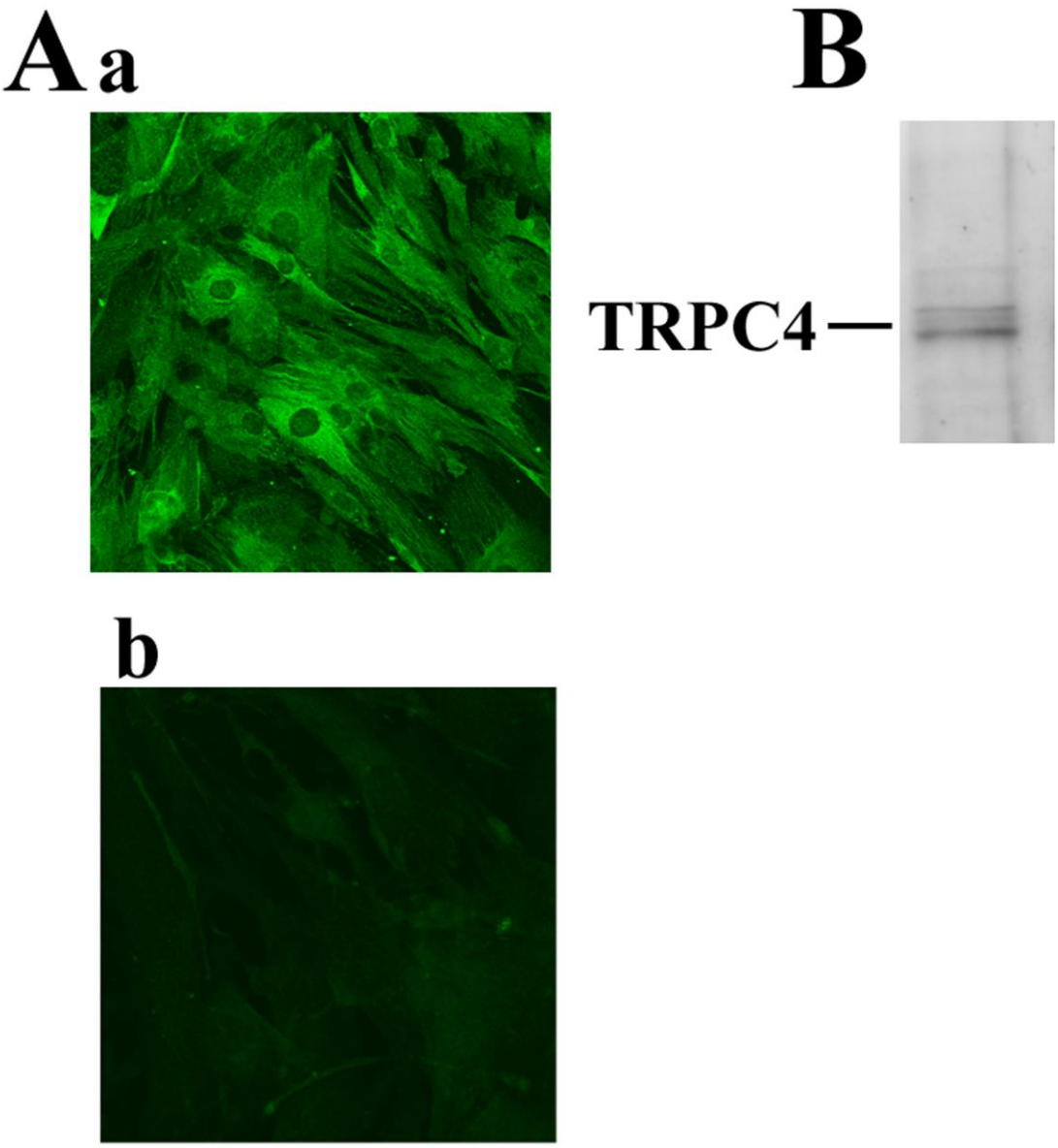

Figure 8. TRPC4 expression in hCASMCs.

Aa: Staining (green) for TRPC4. Ab: Negative control without the antibody (anti-TRPC4).

B: Western blot analysis showing the expression of TRPC4 protein in hCASMCs.

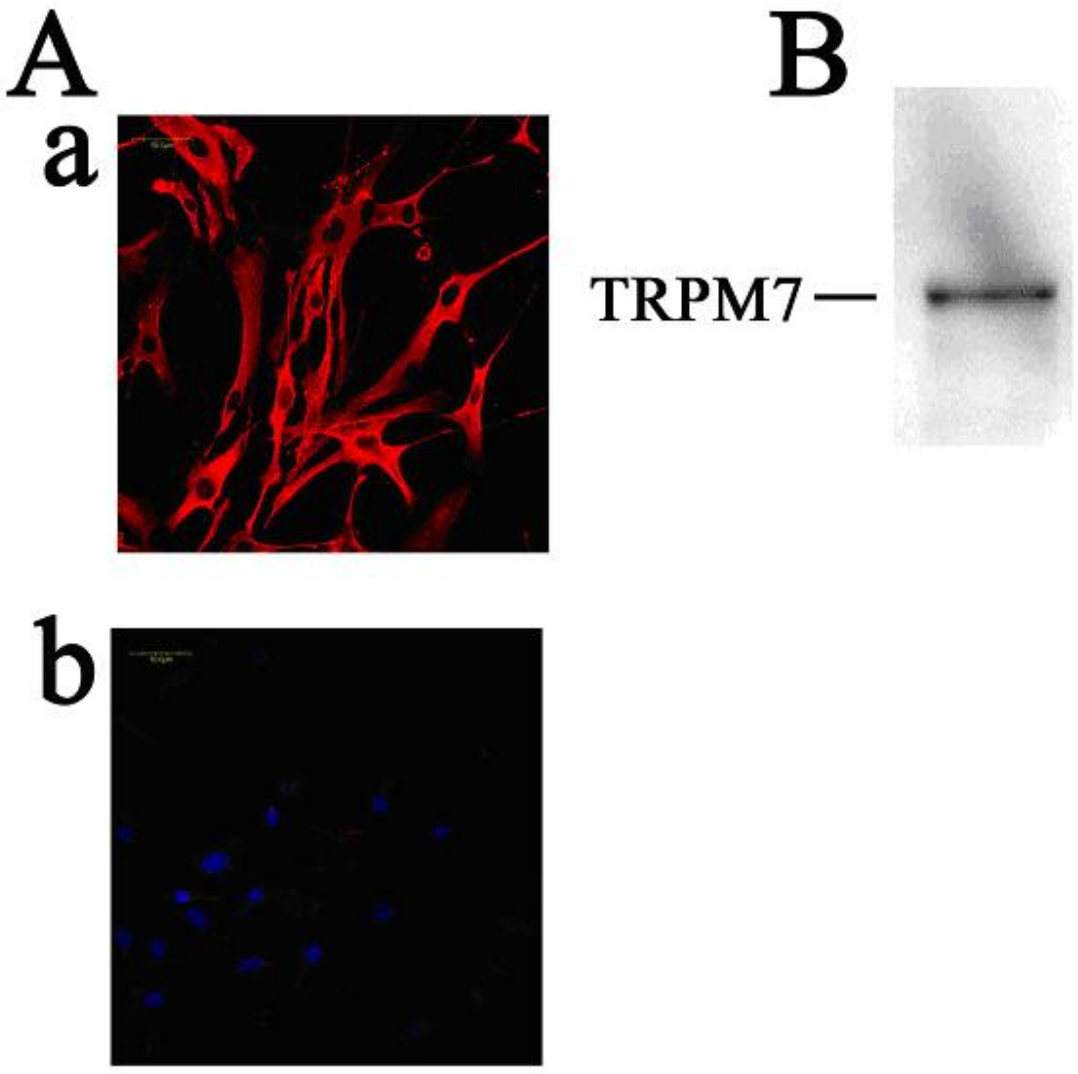

Figure 9. TRPM7 expression in hCASMCs.

Aa: Staining (red) for TRPM7. Ab: Negative control without the antibody (anti-TRPM7). The cells were counterstained with DAPI to visualize nuclei.

B: Western blot analysis showing the expression of TRPM7 protein in hCASMCs.

4-5 Effects of LPC on $[Mg^{2+}]_i$ mobilization in hCASMCs

Magnesium is one of the most abundant intracellular divalent cations and has an important role on the various cell functions as a cofactor for many enzymes and a modulator of intracellular Ca^{2+} concentration, which induce cell contraction, secretion, and proliferation. Among the members of TRP channel families, TRPM6 and TRPM7 are unique channels that play a role as a regulator of cellular Mg^{2+} homeostasis.[32] To determine whether these channels are also activated on hCASMCs, we measured the intracellular Mg^{2+} concentration ($[Mg^{2+}]_i$) by using selective fluorescent probe, mag-fura-2 AM. The effects of SAA and LPC on $[Ca^{2+}]_i$ and $[Mg^{2+}]_i$ were compared, by using fura-2 AM and mag-fura-2 AM as shown in Figure 10. Both SAA (10 μg/ml, Figure 10A) and histamine (100 μM, Figure 10A) increased $[Ca^{2+}]_i$. The subsequent application of LPC (10 μM) markedly increased $[Ca^{2+}]_i$. On the other hand, both SAA and histamine failed to increase $[Mg^{2+}]_i$, while LPC induced a sustained rise in $[Mg^{2+}]_i$ (Figure 10B), proposing that LPC activates Mg^{2+}-permeable channel pathway as well as Ca^{2+} in hCASMCs.

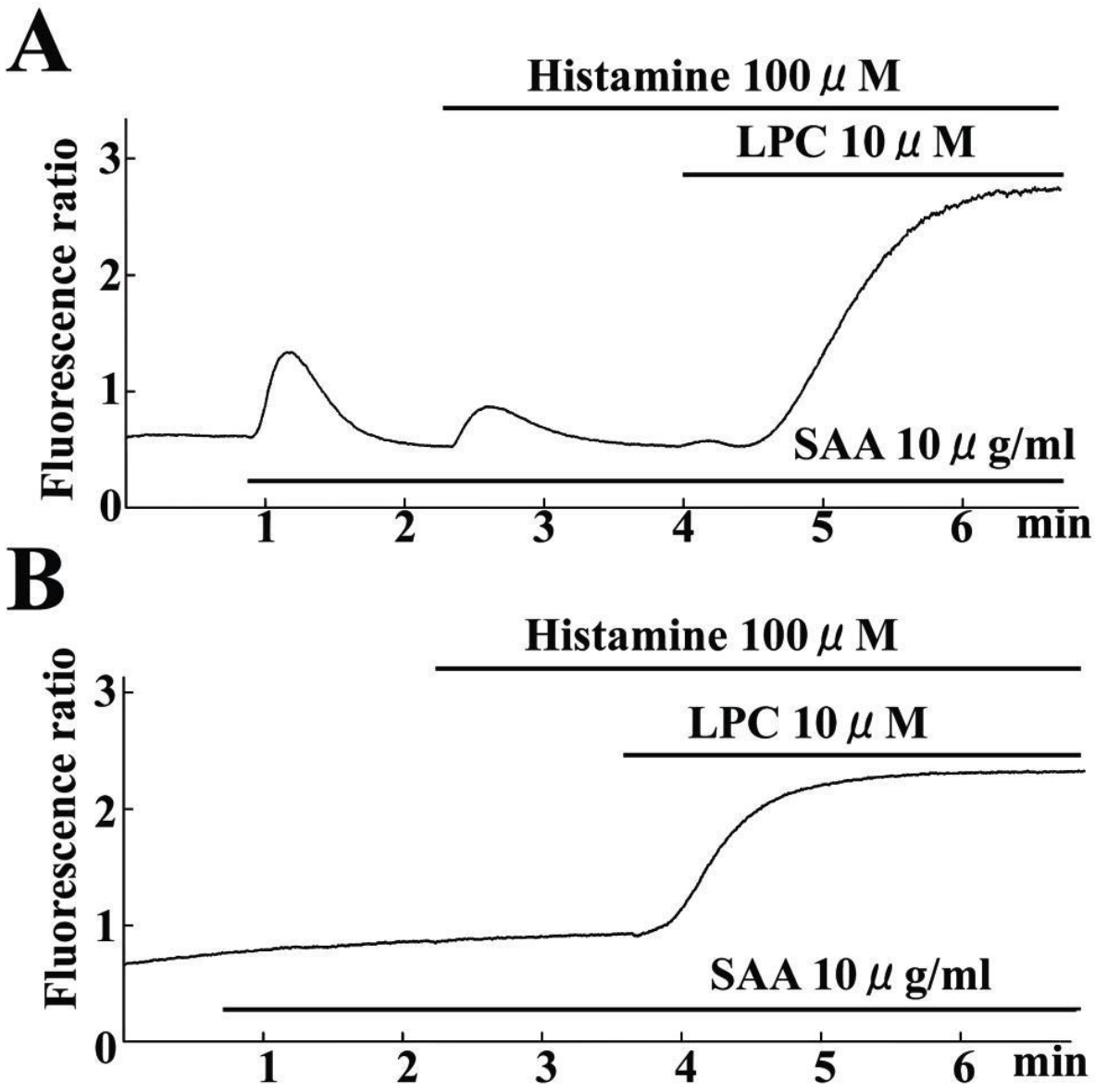

Figure 10. Effects of SAA and LPC on $[Ca^{2+}]_i$ and $[Mg^{2+}]_i$ in hCASMCs.

The effects of SAA and LPC on $[Ca^{2+}]_i$ and $[Mg^{2+}]_i$ were compared, by using fura-2 AM and mag-fura-2 AM. A: Effects of SAA (10 μM), histamine (100 μM) and LPC (10 μM) on $[Ca^{2+}]_i$. B: Effects of SAA (10 μM), histamine (100 μM) and LPC (10 μM) on $[Mg^{2+}]_i$. Note that both SAA and histamine failed to increase $[Mg^{2+}]_i$, while LPC induced a sustained rise in $[Mg^{2+}]_i$. The data were representative of three different experiments.

4-6 Effects of preincubation of pertussis and cholera toxin on $[Ca^{2+}]_i$ mobilization

SAA is known to be coupled to multiple trimetric G proteins.[27,45,46,47] Therefore, I investigated the effects of pertussis toxin (PTX), which selectively inactivates Gi protein on SAA- and LPC-induced Ca^{2+} mobilization in hCASMCs. The cells were pretreated with PTX (Figure 11A, 2 μg/ml) for 2 h, and Ca^{2+} response to SAA (10 μg/ml), histamine (100 μM) and LPC (10 μM) in the presence of extracellular Ca^{2+} was compared with control cells untreated with PTX. As shown in Figure 11A, PTX markedly suppressed SAA-induced Ca^{2+} mobilization (Figure 11Ab), compared with control cells (Figure 11Aa). On the other hand, PTX did not significantly inhibit histamine- and LPC-induced Ca^{2+} mobilization. The data were summarized in Figure 11C. Thus, SAA, but not LPC, appears to activate PTX-sensitive G proteins (Gi), and then Ca^{2+} mobilization in hCASMCs. In addition, the cells were pretreated with cholera toxin (CTX, an activator of Gs protein, 2 μg/ml) for 2 h, and Ca^{2+} response to SAA (10 μg/ml) and histamine (100 μM) in the presence of extracellular Ca^{2+} was compared with control cells. CTX did not affect SAA- and LPC-induced Ca^{2+} mobilization (Figure 11B and 11D).

4-7 Effects of U73122 on SAA- and LPC-induced $[Ca^{2+}]_i$ rise in hCASMCs

In addition, I investigated the effects of U73122, a specific inhibitor of phospholipase C (PLC), which is known to be activated upon Gβγ liberation from trimetric G proteins, on SAA- and LPC-induced Ca^{2+} mobilization in hCASMCs (Figure 12). U73122 abolished the SAA-induced Ca^{2+} mobilization (Figures 12Aa and 12B), compared with control cells (Figure 12Ab). On the other hand, it failed to inhibit LPC-induced Ca^{2+} mobilization (Figures 12Aa, 12Ab and 12B). These results suggest that G protein coupled PLC is required for SAA-induced Ca^{2+} mobilization, but not for LPC-induced Ca^{2+} mobilization in hCASMCs.

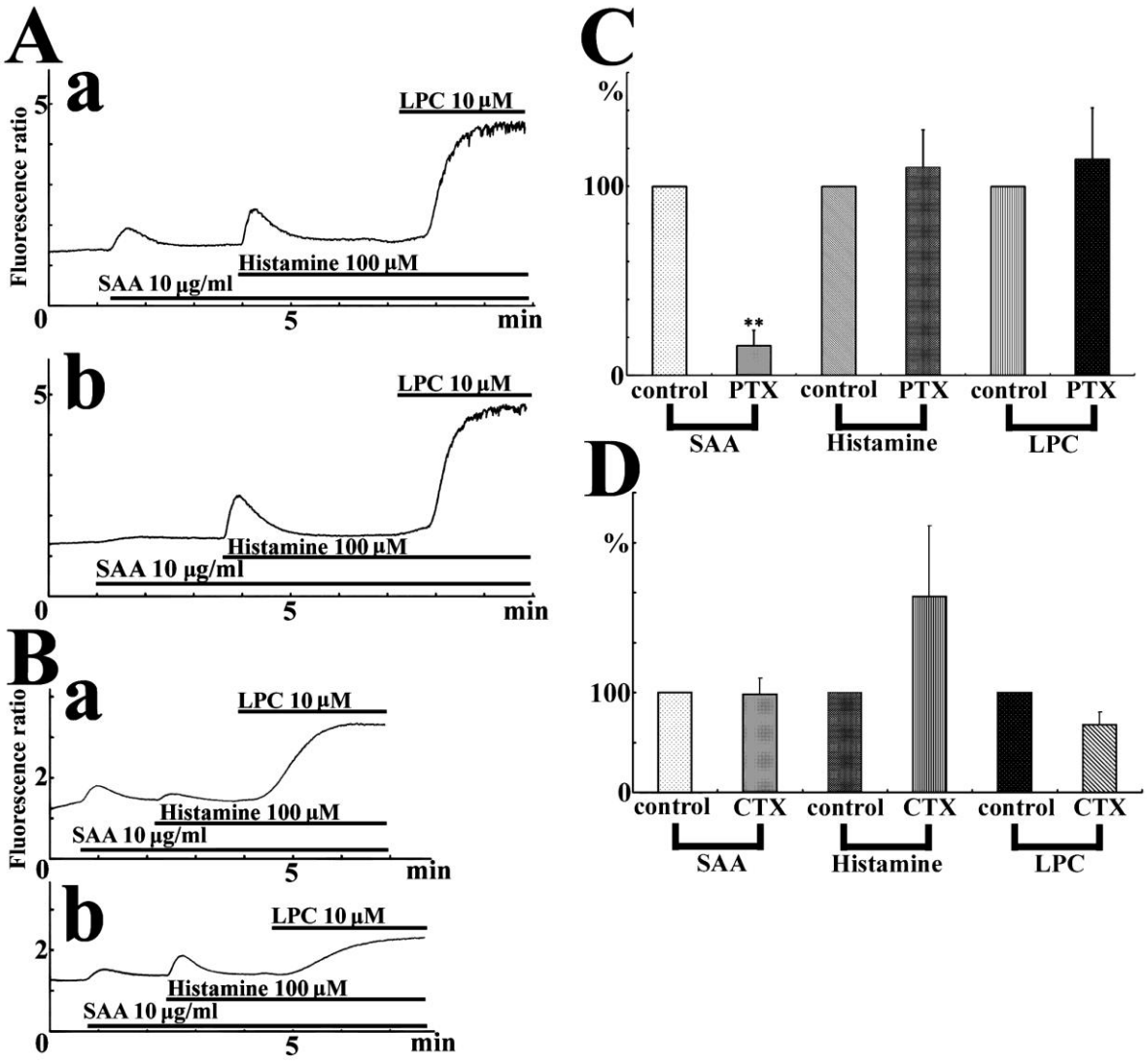

Figure 11. Effects of preincubation of pertussis toxin (PTX) and cholera toxin (CTX) on SAA- and LPC-induced $[Ca^{2+}]_i$ rise.

The cells were pretreated with PTX (A. 2 μg/ml) or CTX (B, 2 μg/ml) for 2 h, and Ca^{2+} response to SAA (10 μg/ml), histamine (100 μM) and LPC (10 μM) in the presence of extracellular Ca^{2+} was compared with the control cells untreated with these agents. The typical data are shown. A: Effects of PTX. a; control cells b, PTX-pretreated cells. Note that PTX markedly suppressed SAA-induced Ca^{2+} mobilization, while PTX did not significantly inhibit histamine- or LPC-induced Ca^{2+} mobilization. B: Effects of CTX. a, control cells b, CTX-pretreated cells. C and D: Effects of PTX and CTX on SAA- and LPC-induced $[Ca^{2+}]_i$ rise. The relative amplitude of SAA-, histamine- and LPC-induced $[Ca^{2+}]_i$ rise is plotted in each drug, compared with control cells (without drug) (C: PTX-pretreated cells, D: CTX-pretreated cells). The data were obtained from three different cells. **P<0.01 vs. control

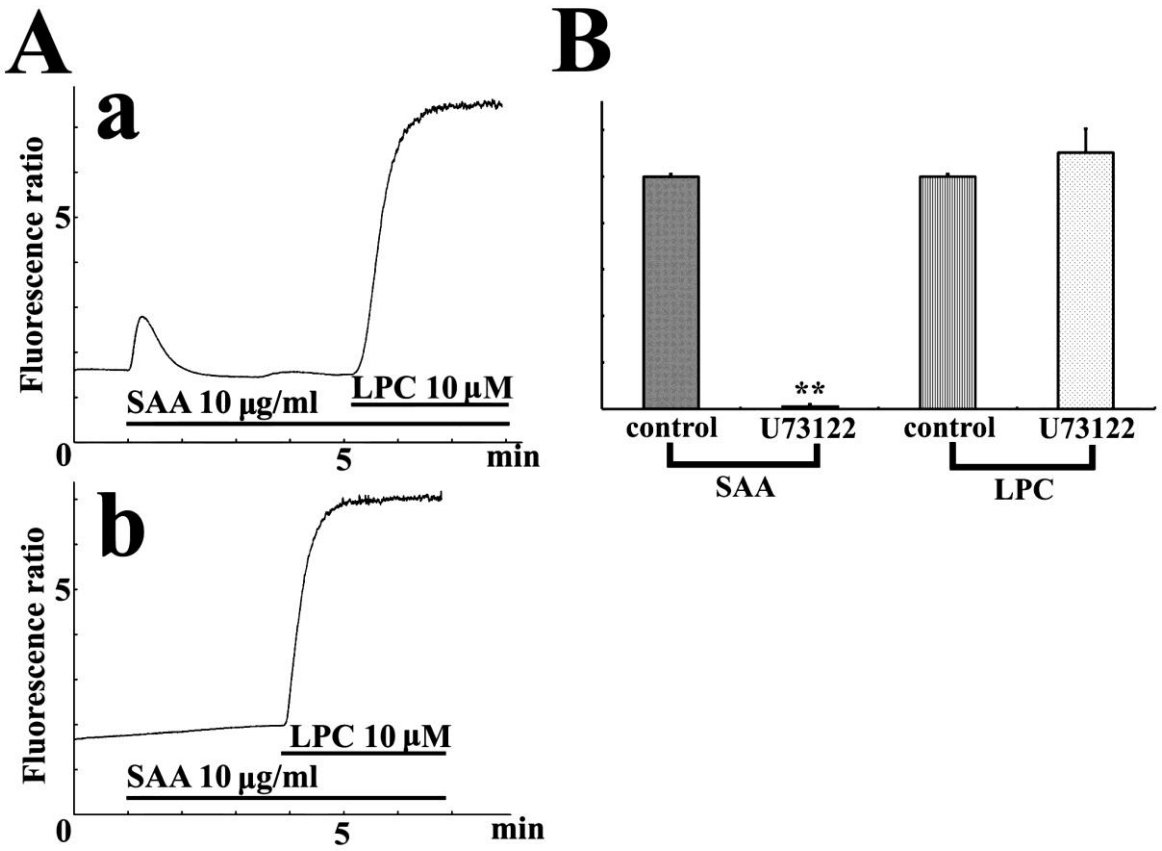

Figure 12. Effects of U73122 on SAA- and LPC-induced Ca^{2+} mobilization in hCASMCs.

The cells were pretreated with U73122 (A. 10 μM) for 10 min, and Ca^{2+} response to SAA (10 μg/ml), and LPC (10 μM) in the presence of extracellular Ca^{2+} was compared with the control cells untreated with U73122. The typical data are shown. Aa: Control cells Ab: Cells pretreated with U73122. Note that SAA failed to increase $[Ca^{2+}]_i$ in U73122 treated cells, but LPC still induced a sustained $[Ca^{2+}]_i$ rise. **P<0.01 vs. control

4-8 Effects of siRNA for TRPC4 on mRNA level and $[Ca^{2+}]_i$ response to SAA in hCASMCs

To determine whether TRPC4 is involved in $[Ca^{2+}]_i$ mobilization induced by SAA on hCASMCs, I investigated the effects of siRNA targeted for TRPC4. After siRNA transfection, the level of TRPC4 mRNA expression was analyzed by real-time quantitative RT-PCR. The expression level of TRPC4 mRNA in hCASMCs transfected with siRNA was significantly decreased, compared with non-coding (negative control) siRNA-treated cells (Figure 13A). In addition, the SAA-induced $[Ca^{2+}]_i$ response was compared in between siRNA-treated cells and non-coding (negative control) siRNA-treated cells. When compared with non-coding siRNA-treated cells, SAA-induced $[Ca^{2+}]_i$ rise was significantly inhibited in cells transfected with siRNA for TRPC4 (Figure 13B and 13C). These results suggested that TRPC4 is involved in SAA-induced calcium influx from extracellular medium in hCASMCs.

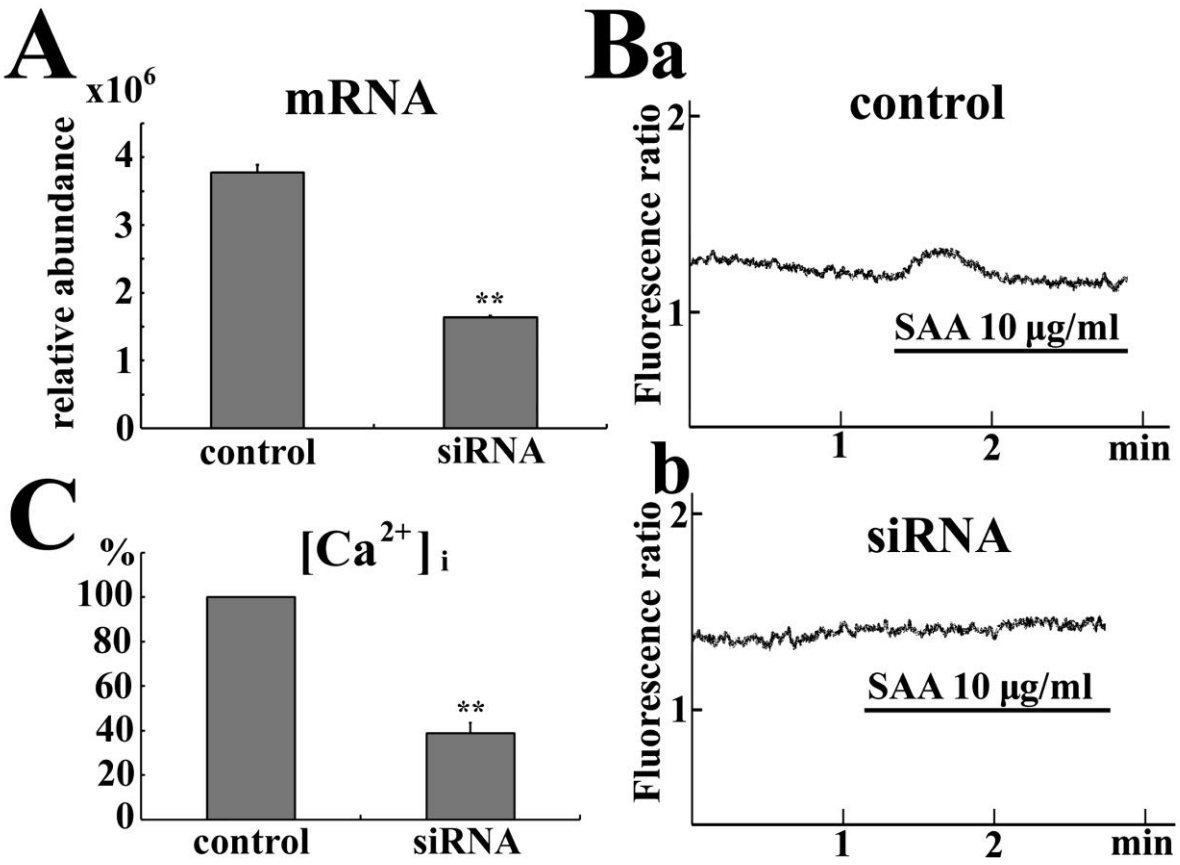

Figure 13. Effects of siRNA targeted for TRPC4 on hCASMCs

A: Effects of siRNA targeted for TRPC4 on expression level of TRPC4 mRNA. HCASMCs have been treated with siRNA targeted for TRPC4 or non-coding control siRNA (n=5).

B and C: The effect of SAA on intracellular calcium mobilization in the cells treated with non-coding control (Ba) and siRNA targeted for TRPC4 (Bb). The calcium mobilization induced by SAA was summarized in Figure C. The $[Ca^{2+}]_i$ rise induced by SAA was markedly inhibited in cells transfected with siRNA for TRPC4. The data were representative of three different experiments. **P<0.01 vs. control

5. Discussion

The major findings of the present study are as follows. 1) Both SAA and LPC increased intracellular calcium concentration ($[Ca^{2+}]_i$) mainly due to calcium influx from extracellular medium in hCASMCs. 2) The SAA-induced Ca^{2+} entry was inhibited by Gd^{3+}, SKF96365 and 2-aminoethoxydiphenyl borate (2-APB), while the LPC-induced Ca^{2+} entry was blocked by Gd^{3+}, but not by SKF96365 and 2-APB. 3) SAA-induced $[Ca^{2+}]_i$ rise required Gi protein and PLC activity, on the contrary, LPC-induced $[Ca^{2+}]_i$ rise required neither G protein nor PLC activity. 3) LPC, but not SAA, increased Mg^{2+} influx as well as Ca^{2+}. 4) The RT-PCR analysis revealed the expression of TRPC1/4, TRPV1/2/4, and TRPM7/8 mRNA. 5) The expression of TRPC1/4, TRPV4 and TRPM7 was confirmed by Western blotting and immunocytochemical analysis. 6) In cells treated with siRNA for TRPC4, the level of TRPC4 mRNA was reduced, and Ca^{2+} response for SAA was significantly attenuated, compared with control cells. These results suggest that SAA/LPC activate Ca^{2+} influx in hCASMCs; SAA activates it via PTX-sensitive G-protein, PLC and TRPC pathways, where TRPC4 may be involved. On the other hand, LPC may activate it independently of these pathways. Thus, TRP protein appears to be a target molecule of Ca^{2+} signaling in hCASMCs elicited by SAA/LPC, which may play roles in coronary muscle remodeling under the pathophysiological and inflammatory conditions such as atherosclerosis.

Transient receptor potential (TRP) channels were initially identified in Drosophila. Later, TRP channels were found in vertebrates. They are ubiquitously expressed in various cell types and play vital roles in regulation of cellular functions such as vasoconstriction and cell proliferation.[42] The existence of TRP channels has also been described in smooth muscle cells.[43] But the molecular identities and function of TRP channels remained quite unexplored

in hCASMCs, and only a few of studies have been reported about expression of TRPC channels. To date, seven TRPC subtypes have been identified: TRPC1 to TRPC7, and classified into four subgroups based on their amino acid sequences: TRPC1, TRPC3/6/7, and TRPC4/5. TRPC2 is a pseudo-gene in humans. Takahashi et al. (2007)[44] reported that hCASMCs using standard RT-PCR analysis constitutively expressed TRPC1, TRPC3, TRPC4, TRPC5, and TRPC6 genes in cultured hCASMCs. In the present study, I confirmed the expression of TRPC1 and TRPC4 among TRPC homologues but failed to detect TRPC3, TRPC5, TRPC6 and TRPC7, which is inconsistent with Takahashi et al. (2007)[44]. The reason of the discrepancy is unclear, but it may be due to the different conditions of cultured cells. In addition, I provided the first evidence showing that TRPV1, TRPV2, TRPV4, TRPM7 and TRPM8 were also detected among TRPV and TRPM homologues in hCASMCs. In addition, among these TRP channels, I confirmed the expression of TRPC1, TRPC4, TRPV4 and TRPM7 protein by Western blotting and immunocytochemical analysis.

A few studies have reported that SAA induces the rise of $[Ca^{2+}]_i$ in human monocytes,[27] and neutrophils.[45] SAA has been also reported to use a receptor that functionally couples to a Gi protein in several cells such as neutrophils.[27,45,46] Badolato et al. (1995)[27] described that SAA induces Ca^{2+} mobilization and chemotaxis by enhancing Ca^{2+} entry in human monocytes, both of which were blocked by pertussis toxin (PTX). PTX selectively mediates adenosine diphosphate (ADP) ribosylation of the Gi class of G proteins, suggesting that the effects of SAA are mediated by a receptor that functionally couples to a Gi protein. On the other hand, it has been reported that SAA induces CCL2 production in human umbilical vein endothelial cells via a PTX-insensitive manner.[47] Thus, multiple signaling pathways may exist in SAA actions. The present study showed that PTX and U73122, an inhibitor of PLC, inhibited Ca^{2+} mobilization induced by SAA, proposing that SAA activates

Ca^{2+} influx pathways via PTX-sensitive G protein (Gi)-PLC pathways in hCASMCs. Kumon et al. (2002)[9] showed that SAA induced cell migration in cultured rat aortic smooth muscle cells, and PTX inhibited it. Since intracellular Ca^{2+} plays an essential role in cell migration, SAA may induce cell migration via enhancing Ca^{2+} mobilization pathway shown in this study. In fact, I observed that SAA enhanced cell migration of hCASMCs (data not shown). Furthermore, I investigated the possibilities of involvement of TRP channels on SAA-induced $[Ca^{2+}]_i$ rise. The voltage-dependent Ca^{2+} channel (L-type and T-type) serves diverse biological functions in vascular smooth muscle cells, and has been reported to be expressed in vascular smooth muscle cells in primary culture.[48] However, neither nifedipine nor mibefradil inhibited SAA-induced Ca^{2+} mobilization, proposing that SAA induces Ca^{2+} mobilization through a non-voltage-dependent Ca^{2+} channel. Alternatively, the compounds Gd^{3+}, SKF96365 and 2-aminoethoxydiphenyl borate (2-APB), a non-selective transient receptor potential (TRP) blocker, inhibited SAA-induced Ca^{2+} mobilization, proposing that the involvement of TRP channels is likely. As mentioned above, I confirmed gene expression of TRPC1/C4, TRPV1/V2/V4 and TRPM7/M8. Moreover, the protein expression of TRPC1/4, TRPV4 and TRPM7 were confirmed by Western blotting and immunocytochemical analysis. 2-APB, which has been reported to inhibit TRPC1, TRPC4 and TRPM8, blocked the SAA-induced $[Ca^{2+}]_i$ rise. In addition, 2-APB, an activator of TRPV1-3,[49] and menthol, an activator of TRPM8, and 4α-phorbol 12,13-didecanoate (4α-PDD), an activator of TRPV4,[50] failed to induce Ca^{2+} mobilization significantly (data not shown). From these observations, it is likely that TRPC1 and/or TRPC4 can be activated by SAA via PTX-sensitive G protein-PLC pathways. Histamine, but not SAA, transiently increased $[Ca^{2+}]_i$ due to Ca^{2+} release from intracellular store sites in the absence of extracellular Ca^{2+}, suggesting that SAA-increased $[Ca^{2+}]_i$ rise was independent of the filling state of internal Ca^{2+} stores, but

dependent on the activation of PLC. Since many studies suggested that TRPC1 is assembled in a Ca^{2+} signaling complex composed of PTX-insensitive Gq subunit,[51] TRPC4 appears to be a target molecule of SAA via PTX-sensitive G protein and PLC pathways. Therefore, I investigated the effects of siRNA targeted for TRPC4. The SAA-induced $[Ca^{2+}]_i$ rise was significantly inhibited in cells treated with siRNA for TRPC4, suggesting that TRPC4 is involved in the SAA-induced $[Ca^{2+}]_i$ mobilization pathway. In fact, it has been reported that TRPC4 can be activated by G protein-coupled receptors.[52,53] Shaefer et al. (2000)[54] showed that TRPC4 forms nonselective cation channels that integrate signaling pathways from G-protein-coupled receptors, and the activity of TRPC4 is dependent on the activation of PLC. The TRPC3/6/7 subfamily of TRPCs has been reported to be activated subsequent to PLC stimulation, either as a result of inositol triphosphate ($InsP_3$)-mediated signaling cascades[55,56] or the lipid second messenger diacylglycerol.[57,58] In contrast to TRPC3/6/7, diacylglycerol does not activate TRPC4. In the present study, 1-oleoyl-2-acetyl-sn-glycerol (OAG), a diacylglycerol analogue, did not increase $[Ca^{2+}]_i$ (data not shown). Thus, the steps leading to channel activation following PLC activation remain unclear, and further studies are also needed to clarify the signaling pathways.

In the present study, LPC slightly increased $[Ca^{2+}]_i$ in the absence of the extracellular Ca^{2+}. These results suggest that LPC induces $[Ca^{2+}]_i$ rise due to the release from the Ca^{2+} storage sites (sarcoplasmic reticulum, SR) as reported previously [59]. However, the addition of Ca^{2+} into the bath solution markedly induced a sustained rise in $[Ca^{2+}]_i$ due to Ca^{2+} entry, suggesting that hat LPC induced Ca^{2+} entry in hCASMCs as reported in rabbit coronary artery smooth muscle cells previously.[30] The previous report suggested that LPC induces Ca^{2+} influx via L-type Ca^{2+} channels.[29] However, in our study, neither nifedipine nor mibefradil blocked Ca^{2+} influx induced by LPC, proposing that LPC induced Ca^{2+} mobilization through a

non-voltage-dependent Ca^{2+} channel. On the other hand, several papers have suggested that LPC activates some types of TRP channels. So et al. (2005)[35] reported that LPC causes an increase of $[Ca^{2+}]_i$ via TRPC6 in cultured human corporal smooth muscle cells. Furthermore, LPC induces migration of monocyte cell line THP-1 requiring TRPC6/TRPV1 activity.[36] LPC can also activate TRPC5 on vascular smooth muscle cells and HEK293 cells over-expressing this channel,[34] and promote TRPM8 channel activity.[60] On the other hand, Monet et al. (2009)[37] supposed that LPC and lysophohphatidylinositol (LPI) stimulate prostate cancer cell migration via TRPV2 channel activation. Thus, the target molecule of LPC on Ca^{2+} entry pathways may be different, depending on cell types or the concentration of LPC used in the study. In this study, to clarify the molecular target of LPC in hCASMCs, I examined the expression of TRP channel family using conventional RT-PCR analysis and Western blotting, Immunocytochemical analysis. In this study, among these TRPC5, TRPC6, TRPV1, TRPV2 and TRPM8, the expression of only TRPV1 and TRPM8 was found in hCASMCs. In addition, OAG (TRPC3/6/7 agonist),[61] 2-APB (TRPV1-3 agonist), 4αPDD (TRPV4 agonist),[50] and menthol, an activator of TRPM8,[62] did not mimic the effects of LPC on Ca^{2+} mobilization (data not shown), proposing that the involvement of TRPV1-4, TRPC3/6/7 and TRPM8 on LPC-induced Ca^{2+} entry is unlikely. In addition, involvement of TRPC1 and TRPC4 was also excluded, because 2-APB blocked SAA-induced Ca^{2+} mobilization, but not LPC effect. Furthermore, LPC caused an increase in Mg^{2+} influx as well as Ca^{2+}. TRPM7 is permeable to both of the divalent cations, Ca^{2+} and Mg^{2+}.[63] Thus, it is very likely that LPC activates Mg^{2+}- and Ca^{2+}-permeable channel pathway in hCASMCs, where TRPM7 may be partly involved. The activation of TRPM7 induced by other substances such as dimethylphytosphingosine and bradykinin has been reported in U937 monocytes and vascular smooth muscle cells.[29,41]

The plasma level of SAA in healthy subjects without acute inflammation is approximately 2–4 μg/ml or less. On the other hand, it may be increased by as much as 1000-fold above its baseline levels, reaching a concentration of 80 μM in acute inflammation recognized as a hallmark of atherosclerotic lesion.[64,65] Johnson et al. (2004)[7] reported that women with definite coronary artery diseases had mean plasma SAA levels of 17.9 μg/ml (ranging from 0.2 to 731 μg/ml), and higher levels of plasma SAA were positively associated with the severity of cardiovascular disease and the risk of cardiovascular events. Thus, the concentrations of SAA used in this study (0.1-10 μg/ml) are clinically relevant. In the present study, SAA induced Ca^{2+} mobilization at concentrations lower than 1 μg/ml, which are near to the plasma level of SAA in healthy subjects without any inflammation. However, SAA in the blood is usually bound to high-density lipoprotein (HDL). And, the effects of SAA including chemotactic activity have been reported to be inhibited by HDL, suggesting that the effects of SAA on hCASMCs shown in the present study may be inactive in circulation.[4] On the other hand, under the pathophysiological and inflammatory conditions where the production of SAA is enhanced, or SAA dissociates from HDL in tissue, the effects of SAA on hCASMCs may be appeared.

On the other hand, LPC increases during ischemia, and the concentration of LPC reaches to 990 μM.[66] In addition, atherosclerotic arteries have been reported to be chronically exposed to high concentration of LPC as compared with normal arteries.[17,18] Wells et al. (1986)[16] reported that the changes of LPC concentrations from 87 to 292 μM tend to parallel the plasma activity levels of LCAT, which are increased when the severity of coronary atherosclerosis increases. Thus, LPC may accumulate under the pathophysiological conditions such as ischemia and atherosclerosis. The present study showed that LPC at concentrations of 3-25 μM induced $[Ca^{2+}]_i$ rise. Thus, the effects of LPC observed in this study may play

significant roles in pathophysiological conditions such as ischemia and atherosclerosis. LPC has been well known to be mainly generated from PLA2-dependent hydrolysis of PC. Recently, Sullivan et al. (2010)[67] reported that SAA increased secretary PLA2 in cultured smooth muscle cells. These observations suggest that SAA may potentiate LPC production in pathophysiological conditions such as ischemia and atherosclerosis.

In conclusion, SAA and LPC activate Ca^{2+} influx in hCASMCs; SAA activates it via PTX-sensitive G-protein, PLC and TRPC pathways, where TRPC4 may be involved. On the other hand, LPC may activate it independently of these pathways. Thus, TRP protein appears to be a target molecule of Ca^{2+} signaling in hCASMCs elicited by SAA/LPC, which may play roles in coronary muscle remodeling under the pathophysiological and inflammatory conditions such as atherosclerosis.

6. Acknowledgement

I would like to express my deep gratitude to my supervisor, Professor Ryozo Nagai and Tatsuya Yamasoba, who supported and encouraged me throughout the research. My sincerest thanks should go to Associate Professor Toshiaki Nakajima for providing me with thoughtful comments on my daily work. I also thank Dr. Imuta and Dr. Hasegawa for teaching and advising me with the daily experiments.

7. References

1) O'Brien KD, Chait A. Serum amyloid A: the "other" inflammatory protein. Curr Atheroscler Rep 2006;8:62-8.

2) Brissette L, Young I, Narindrasorasak S, *et al*. Differential induction of the serum amyloid A gene family in response to an inflammatory agent and to amyloid-enhancing factor. J Biol Chem 1989;264:19327-32.

3) Meek RL, Urieli-Shova S, Benditt P. Expression of apolipoprotein serum amyloid A mRNA in human atherosclerotic lesions and cultured vascular cells: Implications for serum amyloid A function. Proc Natl Acad Sci USA 1994;91:3186-90.

4) Badolato R, Wang JM, Murphy WJ, *et al*. Serum amyloid A is a chemoattractant: induction of migration, adhesion, and tissue infiltration of monocytes and polymorphonuclear leukocytes. J Exp Med 1994;180:203-9.

5) Leinonen E, Hurt-Cameojo E, Wiklund O. Insulin resistance and adiposity correlate with acute-phase reaction and soluble cell adhesion molecules in type 2 diabetes. Atherosclerosis 2003;166:387-94.

6) Tannock LP, O'Brien KD, Knopp RH. Cholesterol feeding increases C-reactive protein and serum amyloid A levels in lean insulin-sensitive subjects. Circulation 2005;111:3057-62.

7) Johnson BD, Kip KE, Marroquin OC, *et al*. Serum amyloid A as a predictor of coronary artery disease and cardiovascular outcome in women: The National Heart, Lung, and Blood Institute-sponsored Women's Ischemia Syndrome Evaluation (WISE). Circulation 2004;109:726-32.

8) Wang X, Chai H, Lin PH, *et al*. Serum amyloid A induces endothelial dysfunction in porcine coronary arteries and human coronary artery endothelial cells. Am J Physiol Circ Physiol 2008;295:H2399-408.

9) Kumon Y, Hosokawa T, Suehiro T, *et al*. Acute-phase, but not constitutive serum amyloid A (SAA) is chemotactic for cultured human aortic smooth muscle cells. Amyloid 2002;9:237-41.

10) Matsumoto T, Kobayashi T, Kamata K. Role of lysophosphatidylcholine (LPC) in atherosclerosis. Curr Med Chem 2007;14:3209-20.

11) Kugiyama K, Sakamoto, Misumi I, *et al*. Transferable lipids in oxidized low-density lipoprotein stimulate plasminogen activator inhibitor-1 and inhibit tissue-type plasminogen activator release from endothelial cells. Circ Res 1993;73:335-43.

12) Xu Y. Sphingosylphosphorylcholine and lysophosphatidylcholine: G protein-coupled receptors and receptor-mediated signal transduction. Biochim Biophys Acta 2002;158:81-8.

13) Sonoki K, Iwase M, Iino K, *et al*. Atherogenic role of lysophosphatidylcholine in low-density lipoprotein modified by phospholipase A2 and in diabetic patients: protection by nitric oxide donor. Metabolism 2003;52:308-14.

14) Zhang B, Fan P, Shimoji E, *et al*. Modulating effects of cholesterol feeding and simvastatin treatment on platelet-activating factor acetylhydrolase activity and lysophosphatidylcholine concentration. Atherosclerosis 2006;186:291-301.

15) Galili O, Versari D, Sattler KJ, *et al*. Early experimental obesity is associated with coronary endothelial dysfunction and oxidative stress. Am J Physiol Heart Circ Physiol 2007;292:H904-11.

16) Wells IC, Peitzmeier G, Vincent JK. Lecithin: cholesterol acyltransferase and lysolecithin in coronary atherosclerosis. Exp Mol Pathol 1986;45:303-10.

17) Portman OW, Soltys P, Alexander M, *et al*. Metabolism of lysolecithin in vivo: effects of hyperlipidemia and atherosclerosis in squirrel monkeys. J Lipid Res 1970;11:596-604.

18) Vidaver GA, Ting A, Lee JW. Evidence that lysolecithin is an important causal agent of atherosclerosis. J Theor Biol 1985;115:27-41.

19) Bergmann SR, Ferguson TB Jr, Sobel BE. Effects of amphiphiles on erythrocytes, coronary arteries, and perfused hearts. Am J Physiol 1981;240:H229-37.

20) Flavahan NA. Atherosclerosis or lipoprotein-induced endothelial dysfunction. Potential mechanisms underlying reduction in EDRF/nitric oxide activity. Circulation 1992;85:1927-38.

21) Chai YC, Howe PH, DiCorleto PE, *et al*. Oxidized low density lipoprotein and lysophosphatidylcholine stimulate cell cycle entry in vascular smooth muscle cells. J Biol Chem 1996;271:17791-7.

22) Chang MY, Tsoi C, Wight TN, *et al*. Lysophosphatidylcholine regulates synthesis of biglycan and the proteoglycan form of macrophage colony stimulating factor. Atherioscler Thromb Vasc Biol 2003;23:809-15.

23) Scalia R, Murohara T, Campbell B, *et al*. Lysophosphatidylcholine stimulates leukocyte rolling and adherence in rat mesenteric microvasculature. Am J Physiol 1997;272:H2584-90.

24) Takahara N, Kashiwagi A, Maegawa H, *et al*. Lysophosphatidylcholine stimulates the expression and production of MCP-1 by human vascular endothelial cells. Metabolism 1996;45:559-64.

25) Kohno M, Yokokawa K, Yasunari K, *et al*. Induction by lysophosphatidylcholine, a major phospholipid component of atherogenic lipoproteins, of human coronary artery smooth muscle cell migration. Circulation 1998;98:353-9.

26) Hsieh CC, Yen MH, Liu HW, *et al*. Lysophosphatidylcholine induces apoptotic and non-apoptotic death in vascular smooth muscle cells: in comparison with oxidized LDL. Atherosclerosis 2000;151:481-91.

27) Badolato R, Johnston JA, Wang JM, *et al*. Serum amyloid A induces calcium mobilization and chemotaxis of human monocytes by activating a pertussis toxin-sensitive signaling pathway. J Immunol 1995;155:4004-10.

28) Zhu X, Learoyd J, Butt S, *et al*. Regulation of eosinophil adhesion by lysophosphatidylcholine via a non-selective-operated Ca^{2+} channel. Am J Respir Cell Mol Biol 2007;36:585-93.

29) Lee YK, Im YJ, Kim YL, *et al*. Characterization of Ca^{2+} influx induced by dimethylphytosphingosine and lysophosphatidylcholine in U937 monocytes. Biochem Biophys Res Commun 2006;348:1116-22.

30) Terasawa K, Nakajima T, Iida H, *et al*. Nonselective cation currents regulate membrane potential of rabbit coronary arterial cell: modulation by lysophosphatidylcholine. Circulation 2002;106:3111-9.

31) Minke B, Cook B. TRP channel proteins and signal transduction. Physiol Rev 2002;82:429-72.

32) Montel C, Birnbaumer L, Flockerzi V. The TRP channels, a remarkably functional family. Cell 2002;108:595-98.

33) Clapham DE. TRP channels as cellular sensors. Nature 2003;426:517-24.

34) Flemming PK, Dedman AM, Xu SZ, *et al*. Sensing of lysophospholipids by TRPC5 calcium channel. J Biol Chem 2006;281:4977-82.

35) So I, Chae MR, Kim SJ, *et al*. Lysophosphatidylcholine, a component of atherogenic lipoproteins, induces the change of calcium mobilization via TRPC ion channels in cultured human corporal smooth muscle cells. Int J Impot Res 2005;17:475-83.

36) Schilling T, Eder C. Non-selective cation channel activity is required for lysophosphatidylcholine-induced monocyte migration. J Cell Physiol 2009;221:325-34.

37) Monet M, Gkika D, Lehen'kyi V, *et al*. Lysophopholipids stimulate prostate cancer cell migration via TRPV2 channel activation. Biochim Biophys Acta 2009;1973:528-39.

38) Grynkiewicz G, Poenie M, Tsien RY. A new generation of Ca^{2+} indicators with greatly improved fluorescence properties. J Biol Chem 1985;260:3440-50.

39) Nakajima T, Okuda Y, Chisaki K, *et al*. Bile acids increase intracellular Ca^{2+}concentration and nitric oxide production in vascular endothelial cells. Br J Pharmacol 2000;130:1457-67.

40) Kishida S, Nakajima T, Ma J, *et al*. Amiodarone and N-desethylamiodarone enhance endothelial nitric oxide production in human endothelial cells. Int Heart 2006;47:85-93.

41) Callera GE, He Y, Yogi A, *et al*. Regulation of the novel Mg^{2+} transporter transient receptor potential melastatin 7 (TRPM7) cation channel by bradykinin in vascular smooth muscle cells. J Hypertens 2009;27:155-68.

42) McFadzean I, Gibson A. The developing relationship between receptor-operated and store-operated calcium channels in smooth muscle. Br J Pharmacol 2002;1351-13.

43) Yip H, Chan WY, Leung PC, *et al*. Expression of TRPC homologs in endothelial cells and smooth muscle layers of human arteries. Histochem Cell Biol 2004;122:553-61.

44) Takahashi Y, Watanabe H, Murakami M, *et al*. Involvement of transient receptor potential canonical 1 (TRPC1) in angiotensin II-induced vascular smooth muscle cell hypertrophy. Atherosclerosis 2007;195:287-96.

45) Bjorkman L, Karlsson J, Karlsson A, *et al*. Serum amyloid A mediates human neutrophil production of reactive oxygen species through a receptor independent of formyl peptide receptor like-1. J Leukoc Biol 2008;83:245-53.

46) He R, Sang H, Ye RD. Serum amyloid A induces IL-8 secretion through a G-protein-coupled receptor, FPRL1/LXA4R. Blood 2003;101:1572-81.

47) Lee HY, Kim SD, Shim JW, *et al*. A pertussis toxin sensitive G-protein-independent pathway is involved in serum amyloid A-induced formyl peptide receptor 2-mediated CCL2 production. Exp Mol Med 2010;42:302-9.

48) Kuga T, Kobayashi S, Hirakawa Y, *et al*. Cell cycle-dependent expression of L- and T-type Ca^{2+} currents in rat aortic smooth muscle cells in primary culture. Circ Res 1996;79:14-9.

49) Hu HZ, Gu Q, Wang C, *et al*. 2-aminoethoxydiphenyl borate is a common activator of TRPV1, TRPV2, and TRPV3. J Biol Chem 2004; 279:35741-8.

50) Watanabe H, Davis JB, Smart D, *et al*. Activation of TRPV4 channels (hVRL-2/mTRP12) by phorbol derivatives. J Biol Chem 2002;277:13569-77.

51) Delmas P. Assembly and gating of TRPC channels in signaling microdomains. Novartis Found Symp 2004;258:75-89.

52) Obukhov AG, Nowycky MC. TRPC4 can be activated by G-protein-coupled receptors and provides sufficient Ca^{2+} to trigger exocytosis in neuroendocrine cells. J Biol Chem 2002;277:16172-8.

53) Jeon JP, Lee KP, Park EJ, *et al*. The specific activation of TRPC4 by Gi protein subtype. Biochem Biophys Res Commun 2008;377:538-43.

54) Schaefer M, Plant TD, Obukhov AG, *et al*. Receptor-mediated regulation of the nonselective cation channels TRPC4 and TRPC5. J Biol Chem 2000;275:17517-26.

55) Kisilevsky R. Serum amyloid A (SAA), a protein without a function: some suggestions with reference to cholesterol metabolism. Med Hypotheses 1991;35: 337-41.

56) Boulay G, Brown DM, Qin N, *et al*. Modulation of Ca^{2+} entry by polypeptides of the inositol 1,4,5-trisphosphate receptor (IP3R) that bind transient receptor potential (TRP): evidence for roles of TRP and IP3R in store depletion-activated Ca^{2+} entry. Proc Natl Acad Sci USA 1999;96:14955-60.

57) Hofmann T, Obukhov AG, Schaefer M, *et al*. Direct activation of human TRPC6 and TRPC3 channels by diacylglycerol. Nature 1999;397:259-63.

58) Okada T, Inoue R, Yamazaki K, *et al*. Molecular and functional characterization of a novel mouse transient receptor potential protein homologue TRP7. Ca^{2+}-permeable cation channel that is constitutively activated and enhanced by stimulation of G protein-coupled receptor. J Biol Chem 1999;274:27359-70.

59) Okajima F, Sato K, Tomura H, *et al*. Stimulatory and inhibitory actions of lysophosphatidylcholine, depending on its fatty acid residue, on the phospholipase C/Ca2+ system in HL-60 leukaemia cells. Biochem J 1998;336:491-500.

60) Abeele FV, Zholos A, Bidaux G, *et al*. Ca^{2+}-independent phospholipase A2-dependent gating of TRPM8 by lysophospholipids. J Biol Chem 2006;281:40174-182.

61) Venkatachalam K, Zheng F, Gill DL. Regulation of canonical transient receptor potential (TRPC) channel function by diacylglycerol and protein kinase C. J Biol Chem 2003;278:29031-40.

62) Andersson DA, Nash M, Bevan S. Modulation of the cold-activated channel TRPM8 by lysophospholipids and polyunsaturated fatty acids. J Neurosci 2007;27:3347-55.

63) Schmitz C, Perraud AL, Johnson CO, *et al*. Regulation of vertebrate cellular Mg^{2+} homeostasis by TRPM7. Cell 2003;114:191-200.

64) Schultz DR, Arnold PI. Properties of four acute phase proteins: C-reactive protein, serum amyloid A protein, alpha 1-acid glycoprotein, and fibrinogen. Semin Arthritis Rheum 1990;20:129-47.

65) Rienhoff HY Jr, Huang JH, Li XX, *et al*. Molecular and cellular biology of serum amyloid A. Mol Biol Med 1990;7:287-98.

66) Corr PB, Snyder DW, Lee BI, *et al*. Pathophysiological concentrations of lysophosphatides and the slow response. Am J Physiol 1982;243:H187-95.

67) Sullivan CP, Seidl SE, Rich CB, *et al*. Secretory phospholipase A2, group IIA is a novel serum amyloid A target gene: activation of smooth muscle cell expression by an interleukin-1 receptor-independent mechanism. J Biol Chem 2010;285:565-75.

Table 1. PCR primers used for amplification of transient receptor potential family genes

Channel (Gene symbol)	Size (bp)		Sequence (`5-`3)
TRPC1	503	sense	TATGGATGTTGCACCTGTCATTT
		antisense	ACTGGGAGACAAACTCTTTCTGG
TRPC3	509	sense	ACGACTTCTACGCTTACGACGAG
		antisense	CTTAATGGCAAGTTTGACACGAC
TRPC4	514	sense	GAGGTACTCTGCCTACTCCCTTCA
		antisense	GAGCCATTGCTTATGTTATGTCTTT
TRPC5	529	sense	CAATGTGAAAGCCAGACACGAAT
		antisense	TCTATTTCCCAAGAGGTCAAGCA
TRPC6	602	sense	TTGACGAAAGTAACATTGGGAGAC
		antisense	ACCAGATTGAAGGGTACAGGAAG
TRPC7	424	sense	TTGTGGAACCTGCTAGATTTCGG
		antisense	GGTTGTATTTGGCACCTCGGTAG
TRPV1	565	sense	GATTGAAGACGGGAAGAATGACT
		antisense	TCTGCCTGAAACTCTGCTTGACC
TRPV2	537	sense	ACATCGCCATTGAGAAGAGGAGT
		antisense	CCACAGAAGCCAGGTCATACAGC
TRPV3	590	sense	ATGCCTGGTTCCACTTTGTCTTT
		antisense	GAATCTGCTCCTCAGCCATTCTG
TRPV4	610	sense	AAAGTCTTCAACCGGCCTATCCT
		antisense	GCAGCAGGTCGTACATCTTGGTA
TRPV5	565	sense	CTGGCTGCCTTGTACCTGCTCTA
		antisense	GACTGGTTGGGTCCTCTGTCTGG
TRPV6	540	sense	ACCTTCGAGCTGTTCCTTACCAT
		antisense	GTTGATTATCCCACGCAGGTCTC

TRPM1	**614**	**sense**	**AAAACTTTCGGACCCTTTACAAC**
		antisense	**AAGAATCCCCATGATAACCTTCA**
TRPM2	**571**	**sense**	**CCTCATCGCCATGTTCAACTACAC**
		antisense	**CTCCTCCGTCTTCTTCCTGCCTC**
TRPM3	**627**	**sense**	**AGAAGGAGGCAGAAGAACCAGAG**
		antisense	**CCACCAGCATAATGATGACAAAG**
TRPM4	**491**	**sense**	**GGCGGAGACCCTGGAAGACA**
		antisense	**TGCGGATGAGCGAGTTGG**
TRPM5	**581**	**sense**	**CTGGACGAGATTGATGAAGCC**
		antisense	**ACGAGCACCGAGCAGTAGTT**
TRPM6	**648**	**sense**	**GGGCAAGTATGGAAATGAAATGA**
		antisense	**ATGGTAAGAAAGCGATGGAGGTT**
TRPM7	**590**	**sense**	**TGTCCCATATCCCACAATCTCAA**
		antisense	**ATCTAGCAAACGCACATACCAAA**
TRPM8	**437**	**sense**	**GCAATGCCATCTCCTACGCTCTA**
		antisense	**GAGTTCTATGTCCATCTCGTCCC**

siRNA (human)

Channel (Gene symbol)		**Sequence (`5-`3)**
TRPC4	**sense**	**CGAAAGGGUUAACCUGCAATT**
	antisense	**UUGCAGGUUAACCCUUUCGTT**
Negative control		**Allstars Negative Control (QIAGEN, cat. No. 1027280)**